AJRCMB Articles in Press. Published on 09-March-2015 as 10.1165/rcmb.2014-0334OC

Duox2-derived Reactive Oxygen Species induce Pattern Recognition Receptors' expression against Influenza A virus in Nasal Mucosa

Hyun Jik Kim[1,5], Chang-Hoon Kim[4,5], Min-Ji Kim[7], Ji-Hwan Ryu[7], Sang Yeop Seong[4], Sujin Kim[7], Su Jin Lim[1], Michael J Holtzman[2,3], Joo-Heon Yoon[4,5,6,7]

[1]Department of Otorhinolaryngology, Seoul National University College of Medicine, Seoul, Korea, [2]Drug discovery program, Pulmonary and Critical Care Medicine, Department of Medicine, [3]Department of Cell Biology, Washington University School of Medicine, St. Louis, Missouri, USA; [4]Department of Otorhinolaryngology, [5]The Airway Mucus Institute, [6]BK 21 Project for Medical Science, [7]Research Center for Natural Human Defense System, Yonsei University College of Medicine, Seoul, Korea;

Running title: Duox2 is required for RIG-I and MDA5 expression

Correspondence to: Joo-Heon Yoon, MD, PhD; Department of Otorhinolaryngology, Yonsei University College of Medicine, 50 Yonsei-ro, Seodaemun-gu, Seoul, Korea 120-752; Tel: 82-2-2228-3610; Fax: 82-2-393-0580; E-mail: jhyoon@yuhs.ac

Author contributions: Conception and design: JHY, HJK; Analysis of data: CHK, MJK, JHR, SYS; Interpretation of data: HJK, SK, SJL; Research advice: MJH; Drafting the manuscript for important intellectual content: HJK.

AJRCMB Articles in Press. Published on 09-March-2015 as 10.1165/rcmb.2014-0334OC

Abstract

We studied the relative roles of Duox2-derived reactive oxygen species (ROS) in host defense against influenza A virus (IAV) infection in normal human nasal epithelial (NHNE) cells and mouse nasal mucosa. We found that Duox2 primarily generated ROS rapidly after IAV infection in NHNE cells, and that knockdown of *Duox2* aggravated IAV infection. In addition, Duox2-derived ROS enhancement significantly suppressed IAV infection in nasal epithelium. In particular, Duox2-derived ROS were required for the induction of retinoic acid-inducible gene 1 (RIG-I), and melanoma differentiation-associated protein 5 (MDA5) transcription. Following intranasal IAV inoculation into mice, viral infection was significantly aggravated from 3 days post-infection (dpi) in the nasal mucosa and the IAV viral titer was highest at 7 dpi. Both RIG-I and MDA5 mRNA levels increased dominantly in mouse nasal mucosa from 3 dpi; consistent with this, RIG-I and MDA5 proteins were also induced after IAV infection. RIG-I and MDA5 mRNA levels were induced to a lower extent in the nasal mucosa of the mice which were inoculated Duox2 shRNA and the IAV viral titer was significantly higher in nasal lavage. Taken together, Duox2-derived ROS are necessary for the innate immune

response and trigger the induction of RIG-I and MDA5 to resist IAV infection in human nasal epithelium and mouse nasal mucosa.

Keywords: Influenza A virus; Duox2; Reactive Oxygen Species; RIG-I; MDA5

AJRCMB Articles in Press. Published on 09-March-2015 as 10.1165/rcmb.2014-0334OC

Introduction

The innate immune system of the respiratory epithelium serves as the first line of defense against invading respiratory viruses. When respiratory epithelium is exposed to viral particles such as single- and double-stranded viral RNA, innate immune mechanisms can be activated to initiate the production of interferon (IFN), a key molecule in antiviral innate immune systems (1, 2). Initiation of these innate immune responses is achieved through the recognition of invading viruses by pattern recognition receptors (PRRs) and virus-derived nucleic acids are considered to activate various PRRs, including members of the membrane-bound Toll-like receptor (TLR) family such as TLR3, 7, and 9, and the recently identified cytoplasmic retinoic acid-inducible gene 1 (RIG-I)-like receptors (RLRs), including RIG-I and melanoma differentiation-associated protein 5 (MDA5) (3). Following the recognition of viral RNAs, the antiviral innate immune response is activated, mainly through the rapid expression of IFNs in nasal epithelium (4). IFNs secreted following viral infection induce antiviral innate immune responses via the Janus kinase/signal transducer and activator of transcription (Jak/STAT) signaling pathway, which facilitates intracellular antiviral signaling through the induction of more than 300 IFN-stimulated genes (ISGs) (4). Reportedly, rapid production of

ISGs could actually be associated with degradation of viral RNA, preventing virus translation and virion assembly, and suppressing viral replication (5, 6).

Influenza A virus (IAV) is a highly contagious agent that causes upper and lower respiratory tract infection, and exhibits tremendous genetic variability through continuous mutations (7). Accordingly, novel influenza strains regularly evolve, to which humans have little immunity, resulting in global pandemics. For this reason, the cure rate of IAV-related pulmonary infectious diseases has not been changed over last years. Therefore, more research is needed to control IAV infection in the respiratory tract, and the identification of new therapeutic inductors represents a critical research goal.

Reactive oxygen species (ROS) are believed to be inevitable toxic by-products that cause cellular damage or stress (8). However, mounting evidence suggests that ROS generation is an important component of the host's arsenal to combat invading microorganisms (9-11). The most common free radical in biological systems is superoxide anion and hydrogen peroxide, products of various oxidative enzymes, including nicotinamide adenine dinucleotide phosphate (NADPH oxidase, Nox). Seven isoforms of Nox (Nox1, Nox2, Nox3, Nox4, Nox5, Duox1, and Duox2) have been identified in human, and Duox has been shown to be the

AJRCMB Articles in Press. Published on 09-March-2015 as 10.1165/rcmb.2014-0334OC

major Nox isoform involved in ROS generation in airway epithelium (8-10). Furthermore, interesting lines of research describe Duox-mediated ROS generation as an integral part of the host defense system at mucosal surfaces (10, 12, 13). Recently, it has been verified that Duox2 is primarily responsible for protection against viral invaders and plays an important role in antiviral innate immunity (14). However, the distinct relationship between Duox2-derived ROS and IFN-related innate immune responses is not fully understood.

Here, we used normal human nasal epithelial (NHNE) cells and an *in vivo* model to clarify the role of Duox2 in acute IAV infection, and investigated how Duox2-derived ROS are responsible for antiviral defense mechanisms. Our data suggest that Duox2 is critical for the generation of key cell surface viral recognition molecules/ PRRs and serves as a host-protective immune response to control acute viral infection in nasal mucosa.

Materials and Methods

More detailed materials and methods may be found in the online supplement.

Cell culture

The Institutional Review Board of the Chung-Ang University College of Medicine approved this study (IRB number C20122095) and all subjects who participated in the study provided written informed consent. Specimens for the culture of NHNE cells were obtained from the middle nasal turbinate of five healthy volunteers. We cultured these specimens using a system designed for normal human nasal epithelial (NHNE) cells (14, 16). Briefly, passage-2 NHNE cells (1×10^5 cells/culture) were seeded in 0.5 ml culture medium on Transwell-clear culture inserts (24.5 mm; 0.45-μm pore size; Costar Co., Cambridge, MA, USA). Cells were cultured in a 1:1 mixture of basal epithelial growth medium and Dulbecco's modified Eagle's medium containing previously described supplements. All the experiments described herein used NHNE cells at 14 days after air-liquid interface formation.

Mice

AJRCMB Articles in Press. Published on 09-March-2015 as 10.1165/rcmb.2014-0334OC

Male C57BL/6J (B6) mice (Orientalbio, Seoul, Korea) aged 7 weeks (19–23g) were used as wild-type (WT) and maintained in our animal facilities under specific, pathogen-free conditions. In vivo experiments were approved by the Institutional Review Board of the Yonsei University College of Medicine (IRB number 2014-0163).

Virus inoculation

NHNE cells were either mock-infected (PBS) or inoculated with IAV (WS/33, H1N1) at a multiplicity of infection (MOI) of 1. IAV (WS/33, H1N1; 213 pfu in 30 μl PBS) was inoculated into mice by intranasal delivery.

Real-time PCR

Total RNA was isolated from NHNE cells and homogenized mouse nasal mucosa infected with WSN/33 (H1N1) at 10 and 30 min, 1, 2, and 8 h, 1, 2, 3, 7, 10, and 14 days using TRIzol (Invitrogen, Carlsbad, CA, USA). cDNA was synthesized from 3 μg of RNA with random hexamer primers using Moloney murine leukemia virus reverse transcriptase (PerkinElmer Life Sciences, Waltham, MA, USA and Roche Applied Science, Indianapolis, IN, USA).

The measurement of ROS

After stimulation with WS/33 (H1N1) for 1 h, confluent cells were washed with RPMI (lacking phenol red). The cells were washed with 1 ml of Hanks' balanced salt solution at least five times to remove mucus secretion, and were then incubated with 5 μM of 2′,7′-DCF-DA for 10 min. Transwell-clear culture inserts were examined with a Zeiss Axiovert 135 inverted microscope equipped with a x20 Neofluor objective and a Zeiss LSM 410 confocal attachment (Minneapolis, MN, USA).

Cell transfection with Nox4, Duox1, and Duox2 shRNAs

Expression of Nox4, Duox1, and Duox2 was suppressed using gene-specific shRNAs (lentiviral particles, Santa Cruz biotechnology, Dallas, Texas, USA), and the transfection rates for shRNAs were determined to be greater than 70% in NHNE cells. The cells were transfected with each shRNA using the Oligofectamine^{TM} reagent following the manufacturer's instructions (Invitrogen, Carlsbad, CA, USA). The shRNA (10 μl, 1×10^4 infectious units of virus) and Oligofectamine^{TM} (1 μg) were mixed individually with the culture media.

AJRCMB Articles in Press. Published on 09-March-2015 as 10.1165/rcmb.2014-0334OC

Duox2 overexpression using full length of cDNA clones

For Duox2 overexpression in NHNE cells, cells were transfected with the Duox2 (NM_177610) and Duoxa2 (NM_025777) mouse cDNA ORF Clones purchased from Origene (Beijing, China).

Duox2 silencing using lentiviral shRNA in mouse nasal mucosa

For Duox2 silencing in mouse nasal mucosa using shRNA lentiviral particles (Thermo Fisher Scientific Inc, Waltham, MA, USA), mice were anesthetized with 50mg/kg Zoletil (Virbac Korea, Seoul, Korea) and 10mg/kg Rompun (Bayer AG, Leverkusen, Germany) and given either mouse Duox2 shRNA (clone ID V3LMM-425530) or scrambled shRNA lentiviral particle ($3x10^7$ TU/ml) twice for three days apart intranasally in a total volume of 30 ul (17). After 6 days, the mice were used for the experiments.

Statistical analyses

At least three independent experiments were performed with cultured cells from each donor, and the results are presented as the mean value ± standard deviation

(SD) of triplicate cultures. Differences between treatment groups were evaluated by analysis of variance (ANOVA) with a *post hoc* test. Differences were considered significant at $p<0.05$.

AJRCMB Articles in Press. Published on 09-March-2015 as 10.1165/rcmb.2014-0334OC

Results

NHNE cells were susceptible to IAV infection.

NHNE cells were obtained from five healthy subjects to assess the susceptibility to IAV and were infected with IAV WS/33 (H1N1) at an MOI of 1. Supernatants and cell lysates were harvested at 10 and 30 min, 1, 2, and 8 h, and 1, 2, and 3 days post-inoculation (dpi). We then measured the mRNA levels of IAV using real-time PCR and found that IAV mRNAs increased significantly from 1 day after infection (mean IAV mRNA: 1.2×10^5 (1 dpi), 1.8×10^6 (2 dpi), 2.2×10^6 (3 dpi), $p<0.05$, Figure 1A). We examined viral titer of IAV by plaque assay and found that viral titer also increased significantly from 1 dpi (2.2×10^5 pfu/ml). Peak titer of IAV was 1.2×10^6 pfu/ml at 3 days after infection ($p<0.05$, Figure 1B). These findings demonstrate the susceptibility of the nasal epithelium to WS/33 (H1N1) and show that the mRNA level and viral titer of IAV increased from 1 day after IAV infection.

Duox2-derived ROS are required for controlling IAV infection

We reported that IAV infection induced intracellular ROS generation at 1 h post-inoculation (hpi) and verified that *Nox4, Duox1*, and *Duox2* mRNA levels increased significantly after IAV infection in nasal epithelium, and the mRNA levels of *Nox1,*

Nox2, Nox3, and *Nox5* were minimally induced by IAV infection (14). Based on these findings, we focused on Nox4, Duox1, and Duox2 as possible Nox subtypes that are involved in IAV-induced ROS generation in nasal epithelium. We then measured the mRNA levels of *Nox4, Duox1*, and *Duox2* using real-time PCR and observed that the mRNA levels of these Nox enzymes increased considerably from 10 min after infection and were maximal at 30 min (*Nox4* mRNA: 32.0±1.1 fold over control, *Duox1* mRNA: 19.4±1.4 fold over control, *Duox2* mRNA: 19.1±0.8 fold over control, $p<0.05$, Figure 2A, 2B, 2C) after IAV infection in NHNE cells.

NHNE cells were transfected with Nox4, Duox1, and Duox2 shRNA to suppress the endogenous mRNA expression of each Nox subtype, and ROS levels were then measured using a fluorescence-based assay with 2′,7′-DCF-DA. Then, plaque assay and western blot analysis were performed to measure the viral titer and IAV nucleoprotein (NP). We found that intracellular ROS generation at 1 hr after IAV infection was significantly attenuated in the cells that were transfected with Duox2 shRNA and the amount of intracellular ROS was not changed in cells transfected with Nox4 and Duox1 (Figure 3A). IAV viral titers in cells (5.9×10^6 pfu/ml) that had been transfected with Duox2 shRNA prior to IAV infection were

AJRCMB Articles in Press. Published on 09-March-2015 as 10.1165/rcmb.2014-0334OC

significantly higher after infection, compared to IAV-infected cells (2.2×10^6 pfu/ml), cells transfected with control shRNA, cells transfected with Nox4 shRNA, and cells transfected with Duox1 shRNA prior to IAV infection (Figure 3B). In addition, western blot analysis also showed that IAV NP expression showed a more considerable increase in Duox2 knockdown cells than in cells showing normal Duox2 expression (Figure 3C).

Subsequently, we transfected the cDNA clones containing the entire pCMV-Duox2 and Duoxa2 sequences into NHNE cells for the enhancement of Duox2-derived ROS. Reverse transcription (RT)-PCR showed that both Duox2 and Duoxa2 mRNA levels were effectively elevated (Figure 3D) and the amount of intracellular ROS was significantly higher in cells overexpressing Duox2 and Duoxa2 at 1 hpi (Duox2 overexpression with IAV infection: 58.9±4.6, only Duox2 overexpression: 24.7±2.7, IAV infection 33.5±1.2 vs. control 5.8±1.6, $p<0.05$, Figure 3E). Interestingly, increased IAV mRNA level (3.6×10^5 vs 3.9×10^4, $p<0.05$, Figure 3F) and NP expression (Figure 3G) at 2 dpi was significantly attenuated in NHNE cells overexpressing Duox2 and Duoxa2. These results indicate that Duox2 is a key mediator, critically important for the generation of ROS and viral load attenuation in NHNE cells. Attenuation of Duox2-derived ROS generation subsequently

aggravated acute IAV infection, and IAV infection could be effectively controlled if the amount of Duox2-derived ROS was increased in the nasal epithelium.

TLR3, RIG-I, and MDA5 are responsible for recognition of IAV in NHNE cells

In order to further evaluate the potential role of Duox2-derived ROS at 1 hpi after IAV infection in nasal epithelium, we examined the relationship between Duox2-derived ROS and the transcription of PRRs after IAV infection.

We infected NHNE cells with WS/33 (H1N1) at MOI 1 and the cell lysates were harvested at 1, 2, and 3 dpi. We then measured the mRNA levels of PRRs, such as TLR3, TLR7, TLR9, RIG-I, and MDA5, which are known to sense double stranded RNA virus in the respiratory epithelium. The results showed that *TLR3*, *RIG-I,* and *MDA5* mRNA levels were significantly induced from 1 dpi, and these levels were maintained up to 3 dpi (Figure 4A). To analyze this in more detail, we determined the levels of transcription for *TLR3*, *RIG-I*, and *MDA5* after IAV infection using real-time PCR. Increased *TLR3, RIG-I,* and *MDA5* gene expression levels were observed from 8 hpi with a peak at 1 dpi (TLR3: 969121.4±551543.3, RIG-I: 3290121.5±282842.7, MDA5: 1214512.3±34648.2 Figure 4B, 4C, 4D). These data suggest that TLR3, RIG-I, and MDA5 are the dominant PRRs

AJRCMB Articles in Press. Published on 09-March-2015 as 10.1165/rcmb.2014-0334OC

responding IAV infection as such are critical components of the innate immune response in nasal epithelium.

Duox2-derived ROS are involved in RIG-I and MDA5-mediated immune response.

To determine the relationship between Duox2-derived ROS and induction of TLR3, RIG-I, and MDA5 transcription after IAV infection, cells were transfected with Duox2 shRNA and then inoculated with IAV WS/33 (H1N1). The mRNA levels of *TLR3, RIG-I,* and *MDA5* were analyzed by real-time PCR at 1 dpi. IAV infection resulted in increased mRNA levels of *TLR3, RIG-I,* and *MDA5* at 1 dpi, and IAV-induced *RIG-I* and *MDA5* mRNA levels decreased significantly in cells with knocked-down Duox2 gene expression compared to cells transfected with control shRNA (RIG-I: 1.3×10^6 vs. 5.1×10^5, MDA5: 3.3×10^6 vs. 1.2×10^6, $p<0.05$). However, *TLR3* mRNA levels were not attenuated in Duox2 knockdown cells (Figure 5A, 5B, 5C). In addition, both *RIG-I* and *MDA5* mRNA levels were considerably elevated in cells with an increased amount of Duox2-derived ROS compared to cells that were infected with IAV (RIG-I: 4.3×10^6 vs. 2.5×10^6, MDA5: 5.6×10^6 vs. 2.4×10^5, $p<0.05$, Figure 5D, 5E). Interestingly, both *RIG-I* and *MDA5* mRNA levels were significantly

higher in Duox2-overexpressing cells without IAV infection than in uninfected cells (RIG-I: 6.1×10^6 vs. 1.2×10^5, MDA5: 7.4×10^6 vs. 1.0×10^5, $p<0.05$). These results provide strong evidence that Duox2-derived ROS are essential for the induction of cytoplasmic PRRs, RIG-I, and MDA5 in nasal epithelium.

Duox2-derived ROS are required for induction of RIG-I and MDA5 in nasal mucosa *in vivo*.

In order to prove whether Duox2 was involved in the induction of RIG-I and MDA5 in nasal mucosa in response to IAV infection, we established an *in vivo* model of acute nasal IAV infection in mice. First, we infected B6 mice (N=3) with IAV WS/33 (H1N1), via the intranasal administration of a dose of 213 pfu. As a gross determinant of virus-induced morbidity, the body weights of the infected WT mice were monitored for 14 day and significant weight loss values were observed from 6 dpi until 12 dpi, compared with uninfected mice (Figure 6A). Then we inoculated 213 pfu IAV WS/33 (H1N1) to B6 mice (N=5) by intranasal delivery and performed the plaque assay using NAL fluid which was obtained at 3, 7, 10, and 14 dpi. The results showed that viral titer was elevated significantly from 3 dpi, and the highest titer was observed at 7 dpi (14200 pfu/ml). Subsequently, the viral titer gradually

AJRCMB Articles in Press. Published on 09-March-2015 as 10.1165/rcmb.2014-0334OC

decreased until 14 dpi (2500 pfu/ml) in IAV infected mice (Figure 6B). Correspondingly, hematoxylin and eosin (H&E)-stained micrographs of coronal nose sections were obtained from WT mice at 0, 7, and 14 dpi; mouse nasal mucosa from 7 dpi revealed severe subepithelial consolidation, larger amount of secretion in nasal cavity, increased epithelium detachment compared with nasal mucosa from mice at 0 dpi (Figure 6C). In particular, polymorphonuclear neutrophils (PMNs) infiltration was dominantly in nasal mucosa at 7 days after IAV infection (Figure 6D). These pathological findings were not observed in the nasal mucosa from mice at 14 dpi. Based on these findings, we conclude that mouse nasal mucosa is susceptible to IAV and that infection is significant as early as 3 dpi. IAV infection reached its peak on day 7 and then declined until day 14 in mice with normal immune responses.

Lastly, we attempted to determine if differentially Duox2-generated ROS were related to the induction of RIG-I and MDA5 in response to IAV infection.

For this study, we transfected both control shRNA (N=5, shCont mice) and Duox2 shRNA (N=5, shDuox2 mice) lentiviral particles by intranasal challenge twice for three days apart and then inoculated 213 pfu IAV WS/33 (H1N1) into mice by intranasal delivery. We did not observe any difference in the survival rate between

shCont mice, shDuox2 mice and wild type mice before IAV infection. However, this was accompanied by a significant decrease in survival rate of shDuox2 mice after IAV infection. Endogenous *Duox2* gene expression on nasal mucosa was decreased by 78% after Duox2 shRNA transfection (shCont mice $2.8x10^5$ vs shDuox2 mice 5.9×10^4, $p<0.05$) and The survival rate of mice transfected with Duox2 shRNA after IAV infection was significantly lower than that of shCont mice at 12 dpi (Figure 7A, 7B). This was accompanied by a significant increase in the mean IAV mRNA level from mouse nasal mucosa (shDuox2 mice 2.3×10^7 vs. shCont mice 5.4×10^6, $p<0.05$, Figure 7C) and in the viral titer from NAL fluid (shDuox2 mice 2.2×10^6 vs. shCont mice 4.7×10^5, $p<0.05$, Figure 7D) at 7 dpi. These data reveal that Duox2 participates in the overall host defense of mouse nasal mucosa during the early stages of IAV infection.

After inoculating B6 mice (N=5) with 213 pfu IAV WS/33 (H1N1) by intranasal delivery, cell lysates from nasal mucosa were harvested at 0, 3, 7, 10, and 14 dpi. We then measured the mRNA levels of *TLR3, TLR7, TLR9, RIG-I* and *MDA5* using real-time PCR and found that the mRNA levels of both *RIG-I* and *MDA5* increased significantly from 3 dpi (RIG-I: 9.9×10^4 vs. 8.8×10^3, MDA5: 3.1×10^5) compared with nasal mucosa from uninfected mice (RIG-I: 8.8×10^3, MDA5:

AJRCMB Articles in Press. Published on 09-March-2015 as 10.1165/rcmb.2014-0334OC

9.1×10^3 $p<0.05$, Figure 7E). The mRNA levels of *TLR3, TLR7*, and *TLR9* were minimally enhanced by IAV inoculation (Figure 7E). The protein expression of both RIG-I and MDA5 were also induced at 3 dpi in cell lysates from mouse nasal mucosa (Figure 7F).

Next, RIG-I and MDA5 gene and protein expression levels were measured with cell lysates from the nasal mucosa of shDuox2 mice and compared with shCont mice. The results revealed that IAV-induced gene expression levels of *RIG-I* (shCont mice 5.5×10^5, shDuox2 mice 7.6×10^4, $p<0.05$) and *MDA5* (shCont mice 1.4×10^6, shDuox2 mice 3.9×10^5, $p<0.05$, Figure 7G), as well as their protein expression levels, were significantly attenuated in the nasal mucosa of shDuox2 mice (Figure 7H). These results suggested that RIG-I and MDA5 are dominant receptors for IAV recognition and Duox2 might be essential for the induction of RIG-I and MDA5 expression levels in mouse nasal mucosa.

Discussion

We found that Duox2 is the dominant source of ROS in response to IAV infection and Duox2-derived ROS are integral mediators of transcription of RLR family genes, including RIG-I and MDA5, which are major components of IAV recognition receptors in the nasal epithelium (Figure 8).

In the respiratory tract, ROS are regarded as one of the pathological components of chronic inflammatory airway diseases, such as asthma, pneumonia, and chronic obstructive pulmonary disease (18-20). Based on this knowledge, some researchers have suggested that faster clearance of ROS could reduce lung damage and improve lung function (21, 22). However, ROS have recently been shown to function as messengers, influencing a variety of immunological processes and enhancing host immunity through prevention of pathogen-induced pro-inflammatory cytokines (23-25). ROS generation by exogenous pathogens has also been established in respiratory epithelial cells, and modulation of ROS was reported to be important for respiratory virus-induced innate immune mechanisms (8, 9, 14). In the present study, we showed that IAV infection increased ROS generation in the human nasal epithelium and IAV infection were aggravated when

AJRCMB Articles in Press. Published on 09-March-2015 as 10.1165/rcmb.2014-0334OC

the functions of enzymes that result in ROS generation were clearly knocked down. Therefore, we aimed to assess how ROS contributed to the immune response against IAV infection in nasal epithelium. We demonstrated that IAV-induced ROS were involved in the activation of IAV recognition receptors, especially RIG-I and MDA5, and scavenging of ROS suppressed the transcription of both receptors following IAV infection in the nasal epithelium. The current findings suggest that the absence of ROS could lead to accelerated IAV infection by impeding the transcription of viral recognition receptors in nasal epithelium. Though little is known about the regulatory mechanisms behind RLRs in the nasal epithelium, we conclude that IAV-induced ROS might be a critical mediator for RIG-I and MDA5 transcription in controlling IAV replication. Therefore, further research on the enzymatic source of IAV-induced ROS generation may promote a greater understanding of the RLR-mediated innate immune response and suggest better therapeutic strategies for acute IAV infection in nasal epithelium.

In particular, the importance of Nox enzymes in innate host defense is exemplified by the role of Nox2 in the generation of high amounts of ROS in phagocytic cells, as part of an anti-bacterial mechanism. However, Duox has been widely appreciated as a critical component for ROS production in the lungs (26-30), and

evidence points to Duox as the main Nox isoform that generates ROS in the apical portion of bronchial epithelial cells (31, 32). We also previously reported that Duox is the most abundant Nox subtype in human nasal epithelium (10). Recent studies suggest that Duox may participate in innate host defense, and it also appears to be involved in protective cellular signaling in response to a defined danger signal, carried out by an intracellular NOD-like receptor system, such as NOD2-mediated antibacterial responses (13, 33). A direct contribution of Duox-derived ROS to the early steps of antiviral host defense has also been reported, and Duox-derived ROS has been shown to reduce the alternative splicing of influenza viral gene segments and cause decreased release of viral particle (34). In the present study, we found that Duox2 is a dominant enzyme in ROS generation after IAV infection in nasal epithelia. In particular, knockdown of Duox2 could aggravate IAV infection in nasal epithelium and the innate immune response would be stronger in Duox2-overexpressed cells. Duox2 gene expression was elevated rapidly after IAV infection and ROS production was initiated in order to activate viral recognition receptors. We suggest that suppression of Duox2-derived ROS or reduction of Duox2 expression inactivates a series of RLR family genes, leading to deterioration of IAV infection. In contrast, overexpression of Duox2 increased ROS

AJRCMB Articles in Press. Published on 09-March-2015 as 10.1165/rcmb.2014-0334OC

generation and enhanced both RIG-I and MDA5 transcription, resulting in activation of the innate immune response against IAV infection in nasal epithelium. The precise molecular patterns of virus replication recognized by RIG-I and MDA5 have been reported, and the elucidation of a role for the RLRs in virus-induced IFN production has been facilitated by the availability of RIG-I-/- and MDA5-/- mice (35, 36). Both RLRs might be dominant receptors for RNA virus that result in the activation of innate immune systems, and initial observations using embryonic fibroblasts and bone marrow-derived DCs generated from these mice revealed striking phenotypes including a failure to produce IFN in response to a variety of viral infections (2, 5). Thus far, three families of PRRs, including RLRs, TLRs, and nucleotide-binding domain and leucine-rich-repeat-containing (NLR), have been identified and shown to be activated in response to IAV pathogens (37). The mechanism by which influenza viral infection triggers the secretion of NLR-induced inflammatory cytokines, such as IL-1β, IL-18, and IL-33, has been clearly reported, and we believe that NLRs might be closely related to inflammasome activation (37, 38). Therefore, we focused on the function of TLRs (TLR3, TLR7, TLR9) and RLRs (RIG-I, MDA5) in enhancing the innate immune response against IAV infection in NHNE cells and *in vivo* nasal mucosa.

Interestingly, we found that Duox2-derived ROS might be involved in RLR signaling to resist IAV infection in human nasal epithelia, and the induction of RIG-I and MDA5 transcription was dominant in mouse nasal mucosa after IAV inoculation. Most importantly, the IAV viral titer was markedly higher in the nasal mucosa or NAL fluid of shDuox2 mice than in shCont mice, and lowered induction of RIG-I and MDA5 expression was observed in the nasal mucosa of shDuox2 mice. Both RIG-I and MDA5 significantly contribute to the response to viral infection and appear to be capable of producing IFNs and previously, we showed that intracellular Duox2-generated ROS contribute to type III IFN secretion against IAV infection in NHNE cells (14). Herein, we discern that Duox2 is primarily involved in the rapid induction of IAV recognition receptors, especially RIG-I and MDA5 and might initiate the innate immune response for the secondary control of IAV infection. A Duox2-mediated innate immune response would be expected if nasal epithelium frequently encounters various viruses, including IAV, and Duox2-derived ROS would be required for IAV sensing in human nasal epithelium or mouse nasal mucosa.

In previous studies, a role of ROS in RIG-I signaling in autophagy has been documented, and ROS were associated with RLR-mediated cytokines production

AJRCMB Articles in Press. Published on 09-March-2015 as 10.1165/rcmb.2014-0334OC

(39, 40). It has not been clearly proved how ROS and Duox2 are responsible for the innate immune response in nasal epithelia and we could not verify the concrete mechanism underlying the ROS-sensitive transcription of RIG-I and MDA5 in nasal epithelium. However, we propose a role for Duox2-derived ROS as a mediator of the antiviral defense mechanism in nasal epithelium and that Duox2 might contribute to the activation of IFN-related innate immune signaling through the induction of cytoplasmic RLRs expression.

In conclusion, our study provides insight that Duox2-derived ROS may be crucial for the clearance of Influenza virus in nasal epithelium. The absence of Duox2 leads to dysregulation of RIG-I and MDA5 expression and impedes efficient innate immunity, which aggravate IAV infection.

Acknowledgement

This work was supported by the National Research Foundation of the Korean Government (Ministry of Science, ICT & Future Planning, MSIP), grant 2007-0056092 (J.H.Y.), National Research Foundation of Korea (NRF) funded by the Ministry of Science, ICT & Future Planning (2012M3A9C5048709) (J.H.Y.), National Research Foundation of Korea(NRF) grant funded by the Korea Government (MSIP) (2014R1A2A01003385) (J.H.Y.) and the Basic Science Research Program through the National Research Foundation of Korea (NRF) funded by the Ministry of Education, Science, and Technology grant 2013R1A1A2011612 (H.J.K.).

AJRCMB Articles in Press. Published on 09-March-2015 as 10.1165/rcmb.2014-0334OC

References

1. Kawai T, Akira S. Pathogen recognition with Toll-like receptors. *Curr Opin Immunol* 2005;17:338-344.

2. Yoneyama M, Kikuchi M, Natsukawa T, Shinobu N, Imizumi T, Miyagishi M, Taira K, Akira S, Fujita T. The RNA helicase RIG-I has an essential function in double-stranded RNA induced innate antiviral responses. *Nat Immunol* 2004;5:730-737.

3. Gitlin L, Benoit L, Song C, Cella M, Gilfillan S, Holtzman MJ, Colonna M. Melanoma differentiation-associated gene (MDA5) is involved in the innate immune response to maramyxoviridae infection in vivo. *PLoS pathogen* 2010;6:e1000734.

4. Garcia-Sastre A, Biron CA. Type I interferons and the virus-host relationship: a lesson in détente. *Science* 2006;312:879-882.

5. Wu S, Metcalf JP, Wu W. Innate immune response to influenza virus. *Curr Opin Infect Dis* 2011;24:235-240.

6. Levy DE, Darnell JE. Stats: transcriptional control and biological impact. *Nat Rev Mol Cell Biol* 2002;3:651-662.

7. Horimoto T, Kawaoka Y. Influenza: lessons from past pandemics, warnings from current incidents. *Nat Rev Microbiol* 2005;3:591-600.

8. Liu T, Castro S, Brasier AR, Jamaluddin M, Garofalo RP, Casola A. Reactive oxygen species mediate virus-induced STAT activation. J Biol Chem 2004; 23:2461-2469.

9. van der Vliet A. NADPH oxidases in lung biology and pathology: Host defense enzymes, and more. *Free Radic Biol Med* 2008;44:938-955.

10. Kim HJ, Kim CH, Ryu JH, Joo JH, Lee SN, Kim MJ, Lee JG, Bae YS, Yoon JH. Crosstalk between platelet-derived growth factor-induced Nox4 activation and MUC8 gene overexpression in human airway epithelial cells. *Free Radic Biol Med* 2011;50:1039-1052.

11. Haller O, Kochs G, Weber F. The interferon response circuit: induction and suppression by pathogenic viruses. *Virology* 2006;344:119-130.

12. Mellqvist UH, Hansson M, Brune M, Dahlgren C, Hermodsson S, Hellstrand K. Natural killer cell dysfunction and apoptosis induced by chronic myelogenous leukemia cells: Role of reactive oxygen species and regulation by histiamine. *Blood* 1999;65:196-204.

13. Lipinski S, Till A, Sina C, Arlt A, Grasberger H, Schreiber S, Rosenstiel P. DUOX2-derived reactive oxygen species are effectors of NOD2-mediated antibacterial responses. J Cell Sci *2009*;122:3522-3530.

14. Kim HJ, Kim CH, Ryu JH, Kim MJ, Park CY, Lee JM, Holtzman MJ, Yoon JH. Reactive Oxygen Species Induce Antiviral Innate Immune Response through IFN-λ Regulation in Human Nasal Epithelial Cells. *Am J Respir Cell Mol Biol* 2013;49:855-865.

AJRCMB Articles in Press. Published on 09-March-2015 as 10.1165/rcmb.2014-0334OC

15. Wang J, Oberley-Deegan R, Wang S, Nikrad M, Funk CJ, Hartshorn KL, Mason RJ. Differentiated human alveolar type II cells secrete antiviral IL-29 (IFN-lambda 1) in response to influenza A infection. *J Immunol* 2009;182:1296-1304.

16. Yoon, JH, Gray T, Guzman K, Koo JS, Nettesheim P. Regulation of the secretory phenotype of human airway epithelium by retinoic acid, triiodothyronine, and extracellular matrix. *Am J Respir Cell Mol Biol* 1997;116:724-731.

17. Kim MJ, Ryu JC, Kwon Y, Lee S, Bae YS, Yoon JH, Ryu JH. Dual oxidase 2 in lung epithelia is essential for hyperoxia-induced acute lung injury in mice. Antioxid Redox Signal. 2014;21:1803-1818.

18. Johnson KR, Marden CC, Ward-Bailey P, Gagnon LH, Bronson RT, Donahue LR. Congenital hypothyroidism, dwarfism, and hearing impairment caused by a missense mutation in the mouse dual oxidase 2 gene, Duox2. *Mol Endocrinol* 2012;21:1593-1602.

19. Rhee SG. H_2O_2, a necessary evil for cell signaling. *Science* 2006;312:1882-1883.

20. Koarai A, Sugiura H, Yanagisawa S, Ichikawa T, Minakata Y, Matsunaga K, Hirano T, Akamatsu K, Ichinose M. Oxidative stress enhances toll-like receptor 3 response to double-stranded RNA in airway epithelial cells. *Am J Respir Cell Mol Biol* 2010;42:651-660.

21. Vlahos R, Stambas J, Bozinovski S, Broughton BR, Drummond GR, Selemidis S. Inhibition of Nox2 oxidase activity ameliorates influenza A virus-induced lung inflammation. *PLoS Pathog* 2011; 7:e1001271.

22. Vlahos R, Stambas J, Selemidis S. Suppressing production of reactive oxygen species (ROS) for influenza A virus therapy. *Trends Pharmacol Sci* 2012;33:3-8.

23. Pollock JD, Williams DA, Gifford MA, Li LL, Du X, Fisherman J, Orkin SH, Doerschuk CM, Dinauer MC. Mouse model of X-linked chronic granulomatous disease, an inherited defect in phagocyte superoxide production. *Nat Genet* 1995;9:202-209.

24. Gao XP, Standiford TJ, Rahman A, Newstead M, Holland SM, Dinauer MC, Liu QH, Malik AB. Role of NADPH oxidase in the mechanism of lung neutrophil sequestration and microvessel injury induced by Gram-negative sepsis: studies in p47phox-/- and gp91phox-/- mice. *J Immunol* 2002;168:3974-3982.

25. Zmijewski JW, Lorne E, Zhao X, Tsuruta Y, Sha Y, Liu G, Abraham E. Antiinflammatory effects of hydrogen peroxide in neutrophil activation and acute lung injury. *Am J Respir Crit Care Med* 2009;179:694-704.

AJRCMB Articles in Press. Published on 09-March-2015 as 10.1165/rcmb.2014-0334OC

26. Bae YS, Choi MK, Lee WJ. Dual oxidase in mucosal immunity and host-microbe homeostasis. *Trends Immunol* 2010;31:278-287.

27. van der Vliet A. NADPH oxidases in lung biology and pathology: Host defense enzymes, and more. *Free Radic Biol Med* 2008;44:938-955.

28. Park HS, Jin DK, Shin SM, Jang MK, Longo N, Park JW, Bae DS, Bae YS. Impaired generation of reactive oxygen species in leprechaunism through downregulation of Nox4. *Diabetes* 2005;54:3175-3181.

29. Mahadev K, Motoshima H, Wu X, Ruddy JM, Arnold RS, Cheng G, Lambeth JD, Goldstein BJ. The NAD(P)H oxidase homolog Nox4 modulates insulin-stimulated generation of H2O2 and plays an integral role in insulin signal transduction. *Mol Cell Biol* 2004;24:1844-1854.

30. Lambeth JD, Kawahara T, Diebold B. Regulation of Nox and Duox enzymatic activity and expression. *Free Radic Biol Med* 2007;43:319-331.

31. Schwarzer C, Marchen TE, Illek B, Fischer H. NADPH oxidase-dependent acid production in airway epithelial cells. *J Biol Chem* 2004;279:36454-36461.

32. Ris-stalpers C. Physiology and pathophysiology of the DUOXes. *Antioxid Redox Signal* 2006;8:1563-1572.

33. Weichart D, Gobom J, Klopfleisch S, Häsler R, Gustavsson N, Billmann S, Lehrach H, Seegert D, Schreiber S, Rosenstiel P. Analysis of NOD2-mediated proteome response to muramyl dipeptide in HEK293 cells *J Biol Chem* 2006;281:2380-2389.

34. Snelgrove RJ, Edwards L, Rae AJ, Hussell T. An absence of reactive oxygen species improves the resolution of lung influenza infection. *Eur J Immunol* 2006;36:1364-1373.

35. Wies E, Wang MK, Maharaj NP, Chen K, Zhou S, Finberg RW, Gack MU. Dephosphorylation of the RNA sensors RIG-I and MDA5 by the phosphatase PP1 is essential for innate immune signaling. *Immunity* 2013;38:437-49.

36. Slater L, Bartlett NW, Haas JJ, Zhu J, Message SD, Walton RP, Sykes A, Dahdaleh S, Clarke DL, Belvisi MG, Kon OM, Fujita T, Jeffery PK, Johnston SL, Edwards MR. Co-ordinated role of TLR3, RIG-I and MDA5 in the innate response to rhinovirus in bronchial epithelium. *PLoS Pathog* 2010;6:e1001178.

37. Allen IC, Scull MA, Moore CB, Holl EK, McElvania-TeKippe E, Taxman DJ, Guthrie EH, Pickles RJ, Ting JP. The NLRP3 inflammasome mediates in vivo innate immunity to influenza A virus through recognition of viral RNA. *Immunity* 2009;30:556-65.

38. Li H, Willingham SB, Ting JP, Re F. Cutting Edge: Inflammasome activation by alum and alum's adjuvant effect are mediated by NLRP3. *J Imminol* 2008;181:17-21.

39. Tal MC, Sasai M, Lee HK, Yordy B, Shadel GS, Iwasaki A. Absence of autophagy results in reactive oxygen species-dependent amplification of RLR signaling. *Proc Natl Acad Sci U S A* 2009;106:2770-2775.

40. Soucy-Faulkner A, Mukawera E, Fink K, Martel A, Jouan L, Nzengue Y, Lamarre D, Vande Velde C, Grandvaux N. Requirement of NOX2 and reactive

AJRCMB Articles in Press. Published on 09-March-2015 as 10.1165/rcmb.2014-0334OC

oxygen species for efficient RIG-I-mediated antiviral response through regulation of MAVS expression. *PLoS Pathog* 2010;6:e1000930.

Figure legends

Figure 1 NHNE cells were susceptible to IAV infection. NHNE cells from five healthy volunteers were inoculated with WS/33 (H1N1) for 10 and 30 min, 1, 2, and 8 h, and 1, 2, and 3 days at an MOI of 1. (A) Real-time PCR showed that the IAV mRNA level was elevated from 1 dpi and was highest at 3 dpi. (B) Plaque assay also showed that viral titer was significantly higher from 1 dpi. Results are presented here as the mean±standard deviation (SD) from five independent experiments (* $p<0.05$ compared with levels in mock-infected cells).

Figure 2 The mRNA levels of three Nox subtypes are preferentially induced to produce ROS after IAV infection. NHNE cells were inoculated with WS/33 (H1N1) for 10 and 30 min, 1, 2, and 8 h, and 1, 2, and 3 days at an MOI of 1. Real-time PCR showed that Nox4 (A), Duox1 (B), and Duox2 (C) mRNA levels are induced from 10 min after infection. Results are presented here as the mean±SD from five independent experiments (* $p<0.05$ compared with mRNA levels in mock-infected cells).

AJRCMB Articles in Press. Published on 09-March-2015 as 10.1165/rcmb.2014-0334OC

Figure 3 Duox2 is mainly involved in IAV-induced Intracellular ROS generation in the nasal epithelium. NHNE cells were transfected with control shRNA, Nox4 shRNA, Duox1 shRNA, and Duox2 shRNA to suppress endogenous mRNA expression for 48 h, and plaque assay was performed to measure changes in IAV viral titers after the suppression of Nox4-, Duox1- and Duox2-induced intracellular ROS generation (A, B). After transfecting control shRNA and Duox2 shRNA into NHNE cells, western blot analysis was performed to measure changes in IAV NP following the suppression of Duox2-derived intracellular ROS generation (C). NHNE cells were transfected with pCMV-Duox2 and Duoxa2 overexpression vectors to enhance Duox2-derived intracellular ROS. RT-PCR showed that both Duox2 and Duoxa2 mRNA levels were significantly induced (D) and the amount of intracellular ROS also increased (E) after transfection with Duox2 and Duoxa2 overexpression vectors. Plaque assay and western blot analysis were performed to measure changes in IAV viral titers (F) and IAV NP (G) after the enhancement of Duox2-derived intracellular ROS. The fluorescence intensity and western blot analysis data are representative of five independent experiments, and results are presented here as the mean±SD from five independent experiments (* $p<0.05$

compared with levels in IAV-infected cells or cells transfected with control shRNA or pCMV vector).

Figure 4 The mRNA levels of TLR3, RIG-I, and MDA5 are preferentially induced to recognize IAV in nasal epithelium. NHNE cells were inoculated with WS/33 (H1N1) for 10 and 30 min, 1, 2, and 8 h, and 1, 2, and 3 days; at an MOI of 1. RT-PCR (A) and real-time PCR showed that TLR3 (A), RIG-I (B), and MDA5 (C) mRNA levels are induced from 8 h after infection. Results are presented here as the mean±SD from five independent experiments (* $p<0.05$ compared to mRNA levels in mock-infected cells).

Figure 5 The transcription of RIG-I and MDA5 is preferentially augmented by Duox2-derived ROS after IAV infection. NHNE cells were transfected with control shRNA and Duox2 shRNA, and real-time PCR was performed to measure changes in IAV-induced TLR3 (A), RIG-I (B), and MDA5 (C) gene expression. IAV-induced RIG-I and MDA5 mRNA levels were significantly attenuated in cells transfected with Duox2 shRNA. IAV-induced TLR3 mRNA levels were not changed following the suppression of Duox2-derived intracellular ROS in NHNE

AJRCMB Articles in Press. Published on 09-March-2015 as 10.1165/rcmb.2014-0334OC

cells. The gene expression levels of both RIG-I (E) and MDA5 (F) were considerably elevated in cells in which Duox2-derived ROS levels were increased through the use of Duox2 and Duoxa2 overexpression vectors. The results are presented here as the mean±SD from five independent experiments (* $p<0.05$ compared with levels in IAV-infected cells or cells transfected with control shRNA or pCMV vector).

Figure 6 IAV infection *in vivo*. Wild type mice were infected with 213 pfu IAV WS/33 (H1N1) and assessed for loss of body weight (A) (circle: no infection mice, N=3, triangle: infection mice, N=3) and viral titer from NAL fluid of infected mice (N=5) (B) over the post-infection period. H&E micrographs of nose (coronal) sections obtained from WT mice infected with 213 pfu IAV on days 0, 7 and 14. The H&E micrographs are representative of nose sections from five mice (C) and PMNs were counted in subepithelium of nasal mucosa (D). The results are presented here as the mean±SD from the NAL fluid from five mice (R: right, L: left, S: septum).

Figure 7 IAV infection is enhanced in Duox2 mutant mice and Duox2-induced ROS are required for inducing IAV recognition receptors. WT mice were pretreated with Control shRNA (shCont mice, N=5) or Duox2 shRNA (shDuox2 mice, N=5) and mice infected with 213 pfu IAV WS/33 (H1N1) were assessed for *Duox2* gene expression on nasal mucosa (A) and survival rate over the post-infection period (B). Cell lysates from mice nasal mucosa and NAL fluid were obtained at 7 dpi and real-time PCR and plaque assays were performed to compare viral mRNA levels (C) or viral titers (D) between shCont mice and shDuox2 mice (white dot: shCont mice, black dot: shDuox2 mice).

WT mice (N=5) infected with 213 pfu IAV WS/33 (H1N1) were assessed for mRNA levels of TLR3, TLR7, TLR9, RIG-I, and MDA5, and cell lysates of mice nasal mucosa and NAL fluid were obtained at 3, 7, 10, and 14 dpi (E) (white bar: TLR3, light gray bar: TLR7, gray bar: TLR9, Dark gray bar: RIG-I, black bar: MDA5). Real-time PCR showed that both RIG-I and MDA5 mRNA levels were significantly induced following IAV infection in the mouse nasal mucosa. Western blot analysis was also performed using cell lysates to compare RIG-I and MDA5 protein expression levels at 7 dpi (F) (white bar: RIG-I, black bar: MDA5). shDuox2 mice (N=5) were infected with 213 pfu IAV WSN/33 (H1N1) and were assessed for RIG-

AJRCMB Articles in Press. Published on 09-March-2015 as 10.1165/rcmb.2014-0334OC

I and MDA5 mRNA levels using real-time PCR (G) and protein levels using western blot analysis (H) at 7 dpi. Western blot analysis results are representative of five mice, and PCR results are presented here as the mean±SD from five independent experiments (* $p<0.05$ compared with levels in shCont mice and shDuox2 mice).

Figure 8. Schematic picture of the innate immune response against IAV infection in nasal epithelial cell. IAV infection triggers Duox2-derived and mitochondrial ROS generation resulting in mediating IFN-β and λ secretion in NHNE cells. In particular, Duox2-derived ROS are primarily involved in the rapid induction of IAV recognition receptors, especially RIG-I and MDA5 and Duox2-derived ROS would be necessary for IAV sensing in human nasal epithelium.

AJRCMB Articles in Press. Published on 09-March-2015 as 10.1165/rcmb.2014-0334OC

Figure 1

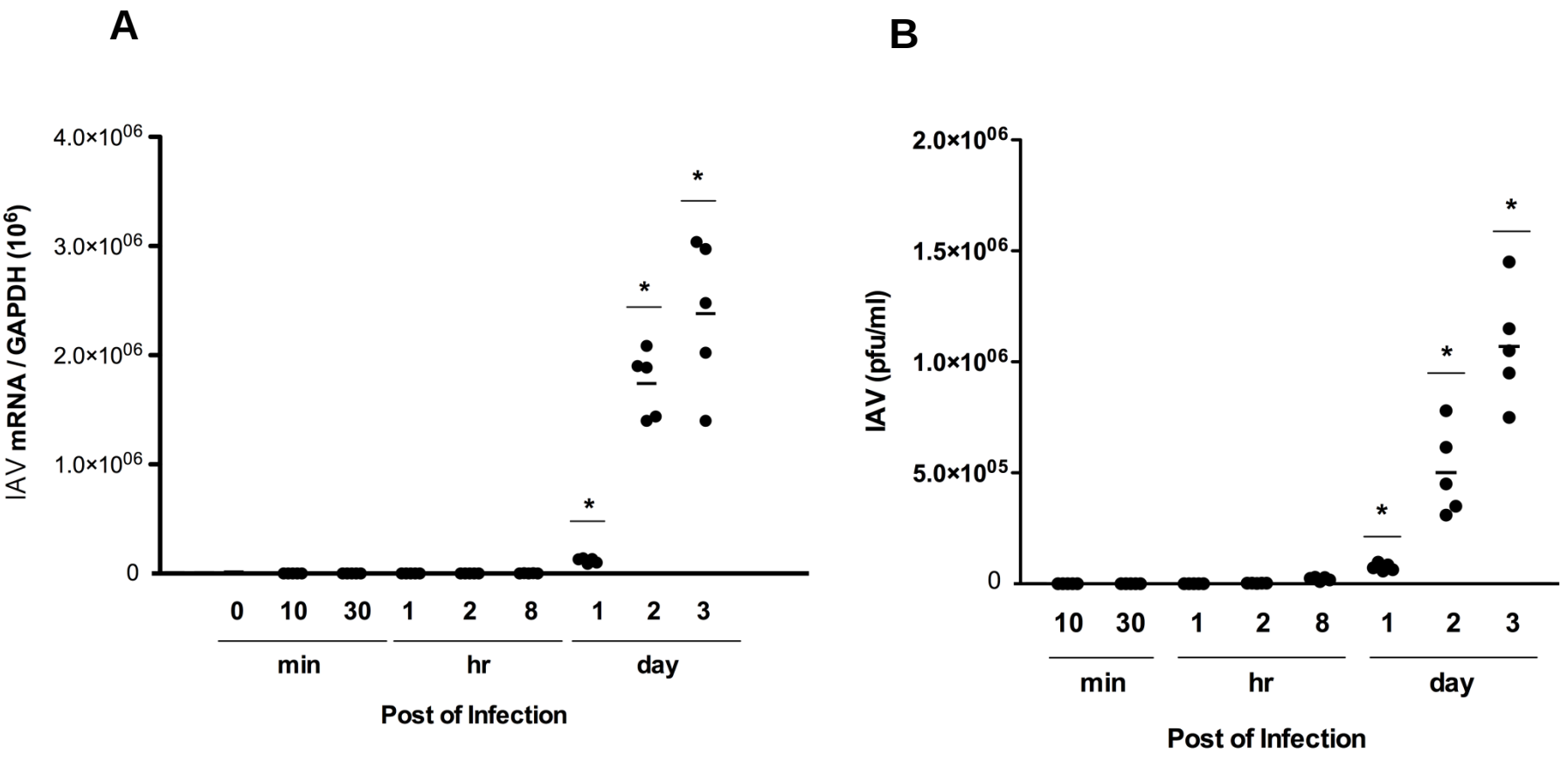

AJRCMB Articles in Press. Published on 09-March-2015 as 10.1165/rcmb.2014-0334OC

Figure 2

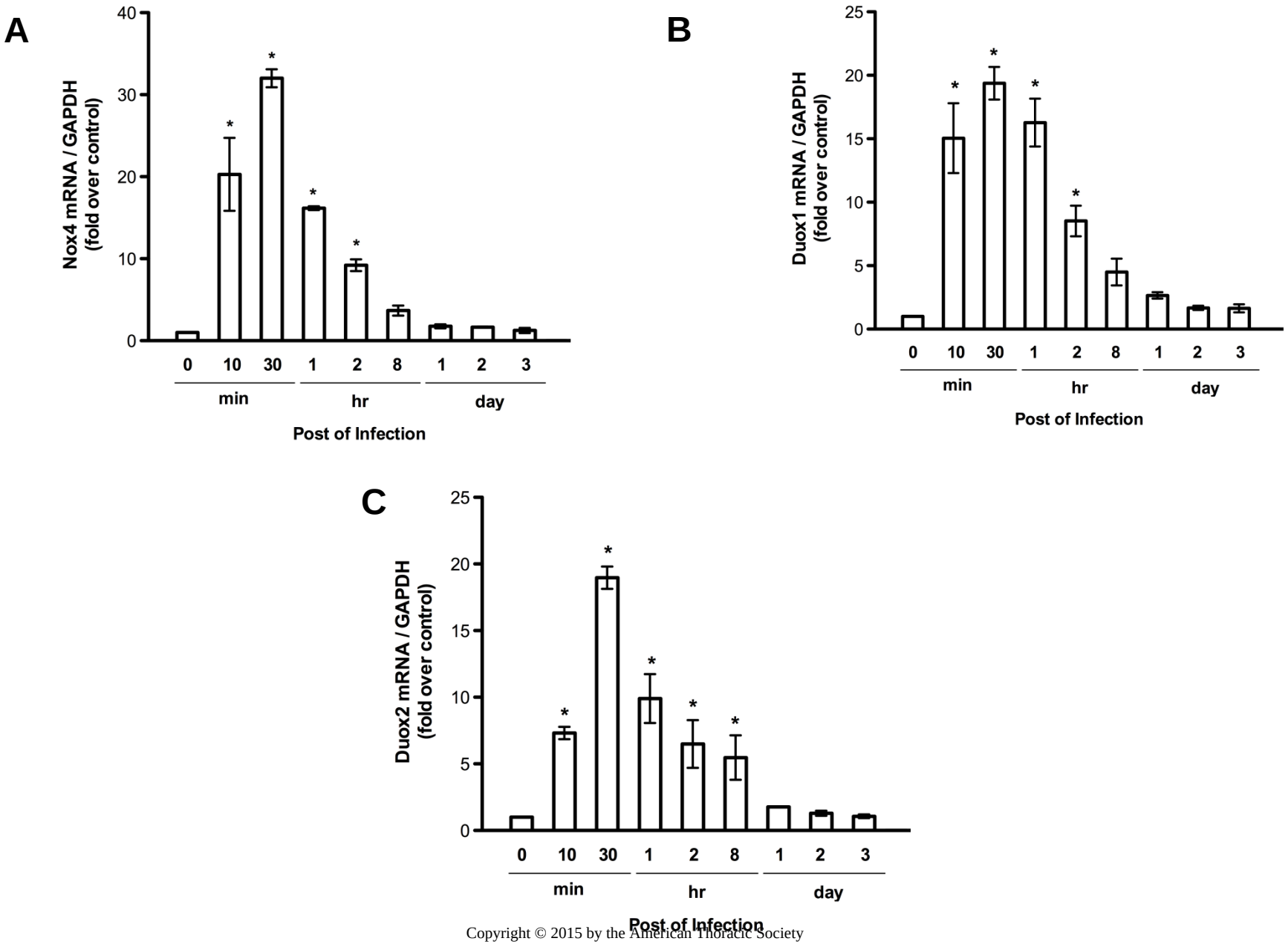

Figure 3

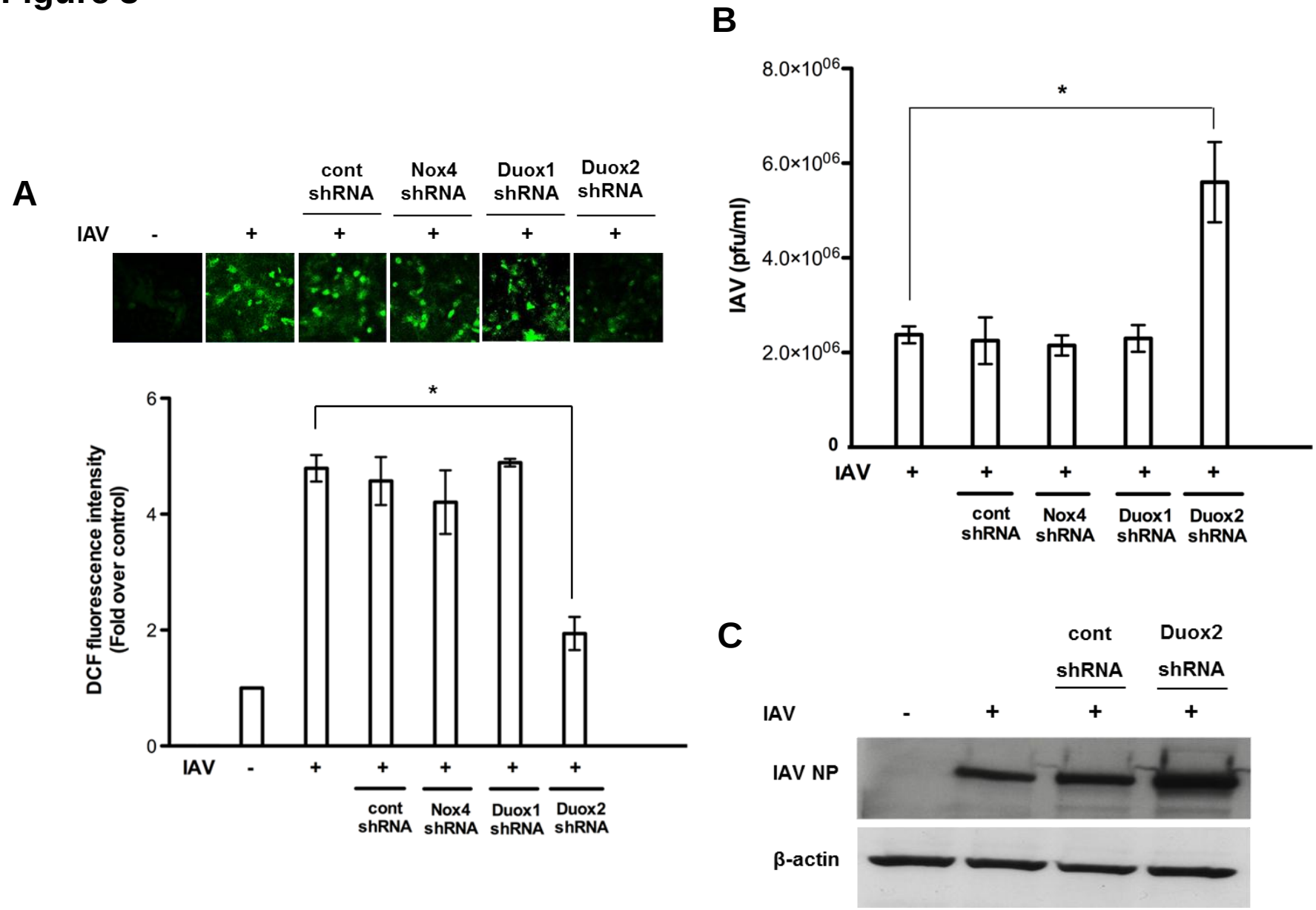

AJRCMB Articles in Press. Published on 09-March-2015 as 10.1165/rcmb.2014-0334OC

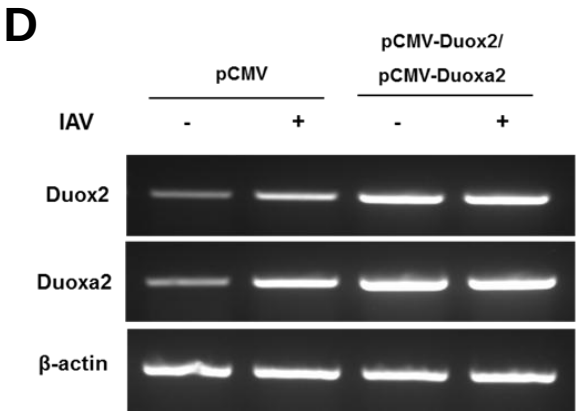

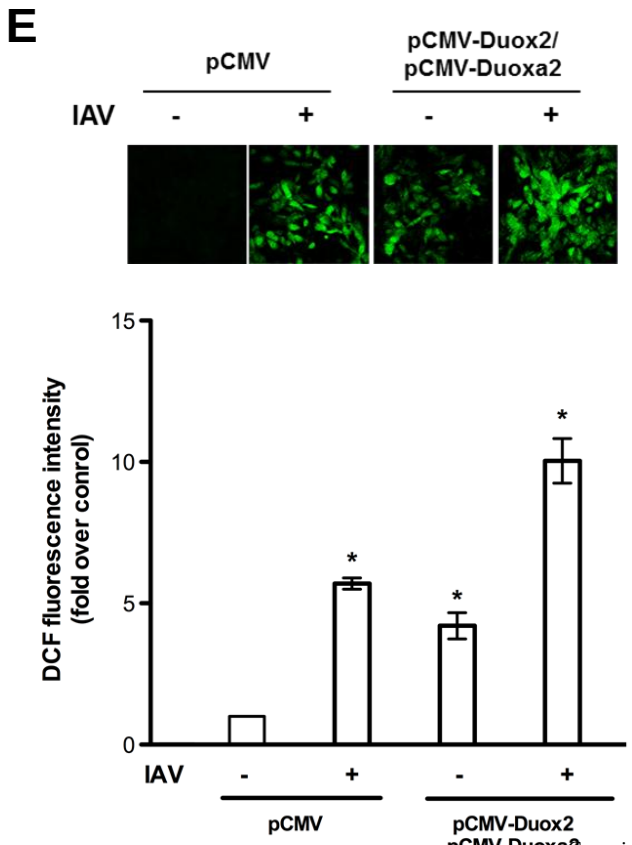

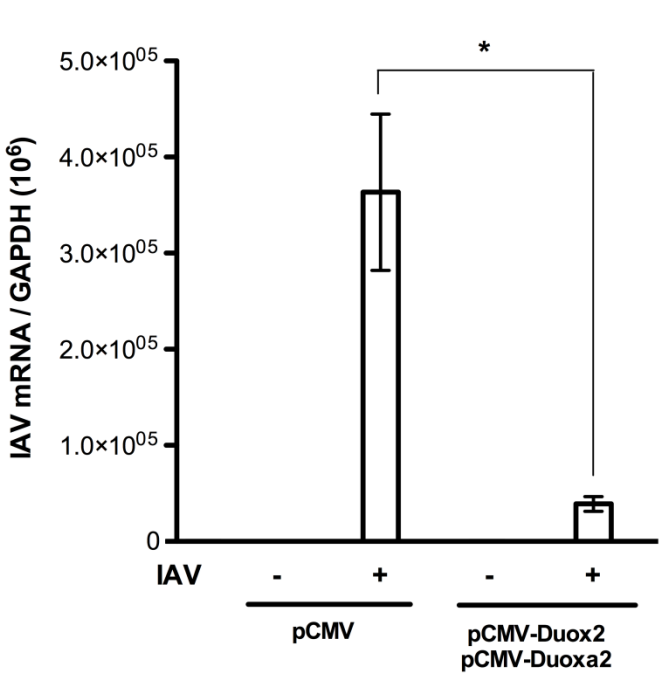

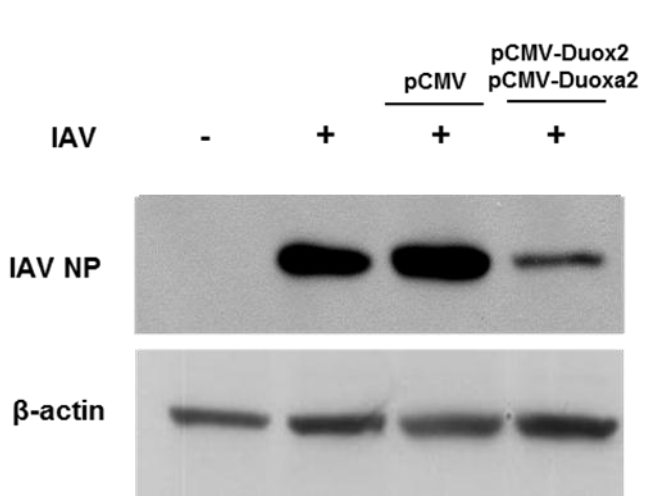

Figure 4

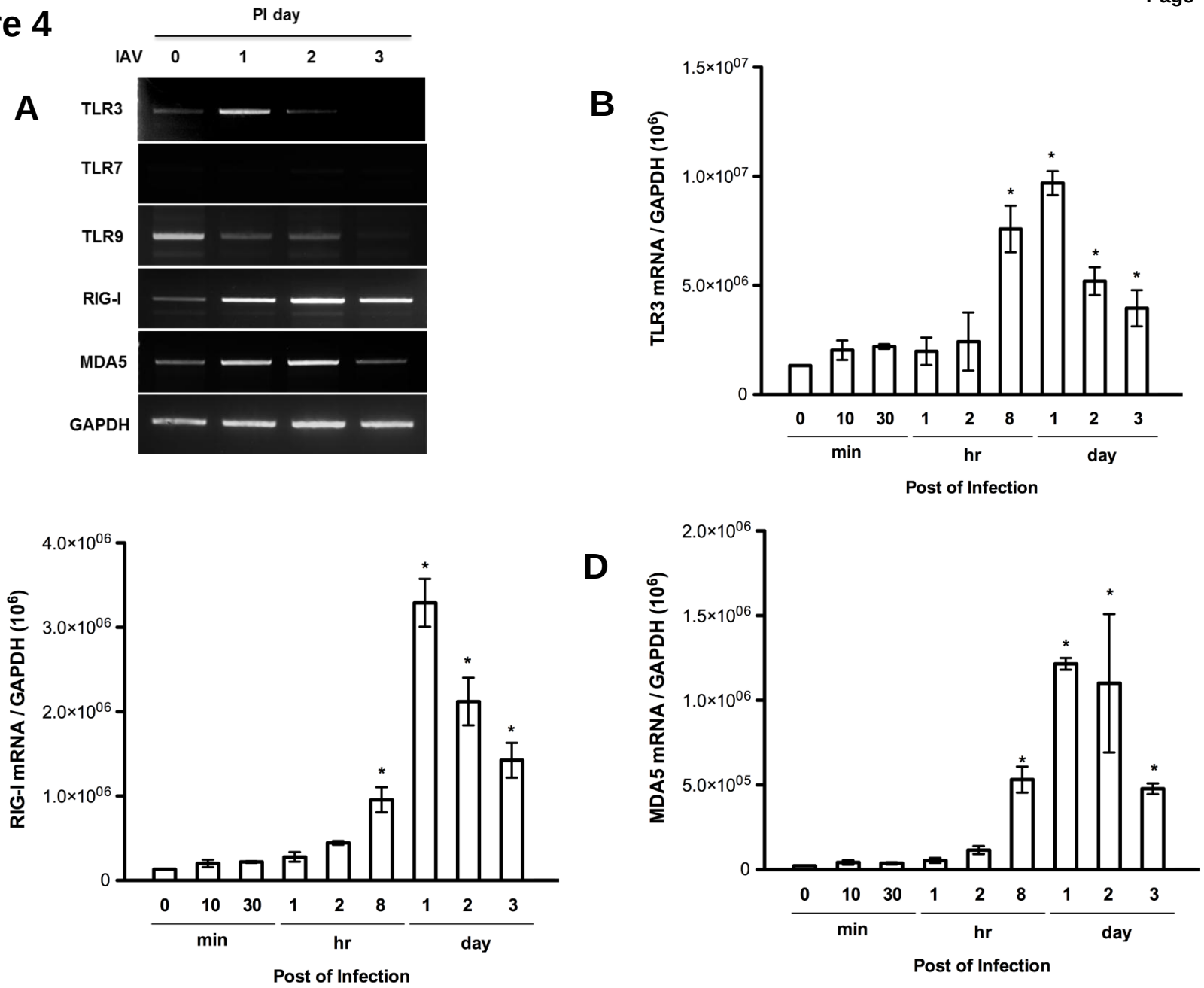

AJRCMB Articles in Press. Published on 09-March-2015 as 10.1165/rcmb.2014-0334OC

Figure 5

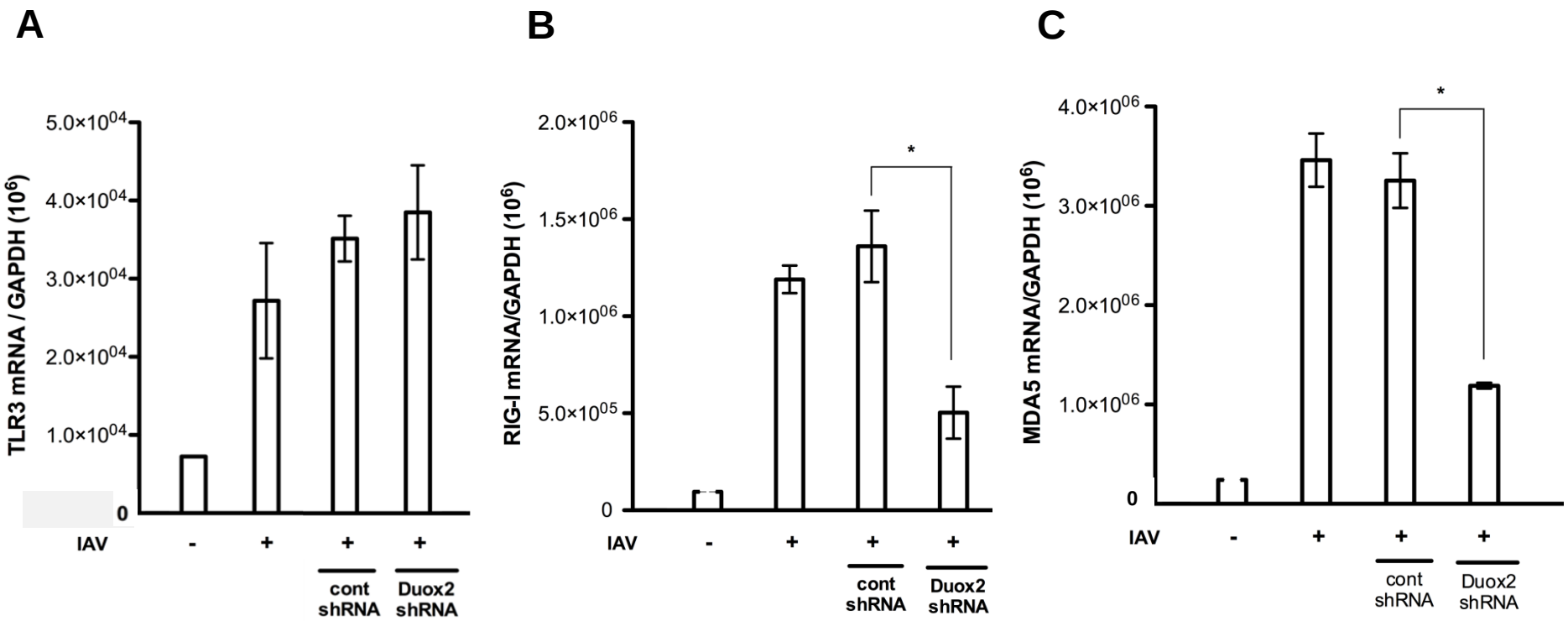

Figure 5

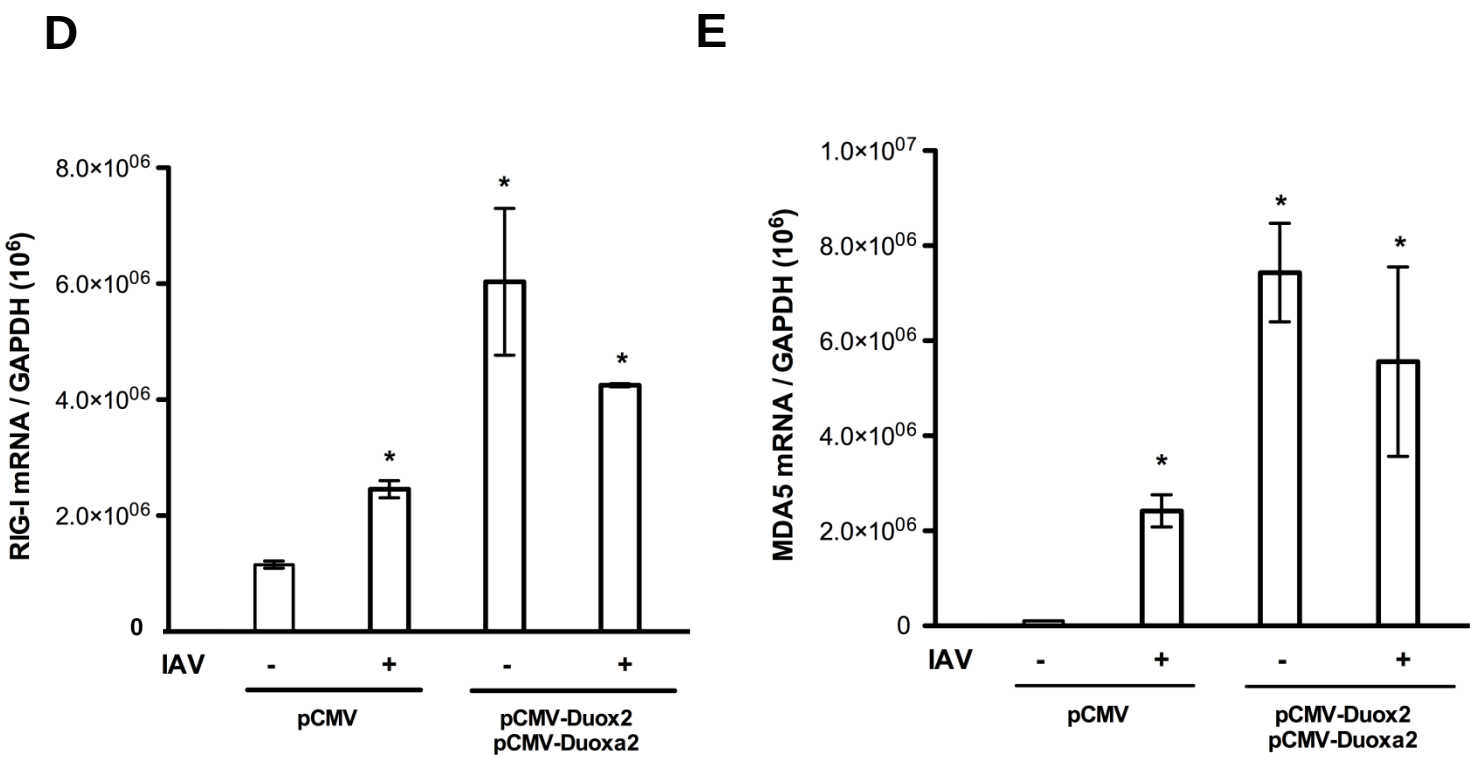

AJRCMB Articles in Press. Published on 09-March-2015 as 10.1165/rcmb.2014-0334OC

Figure 6

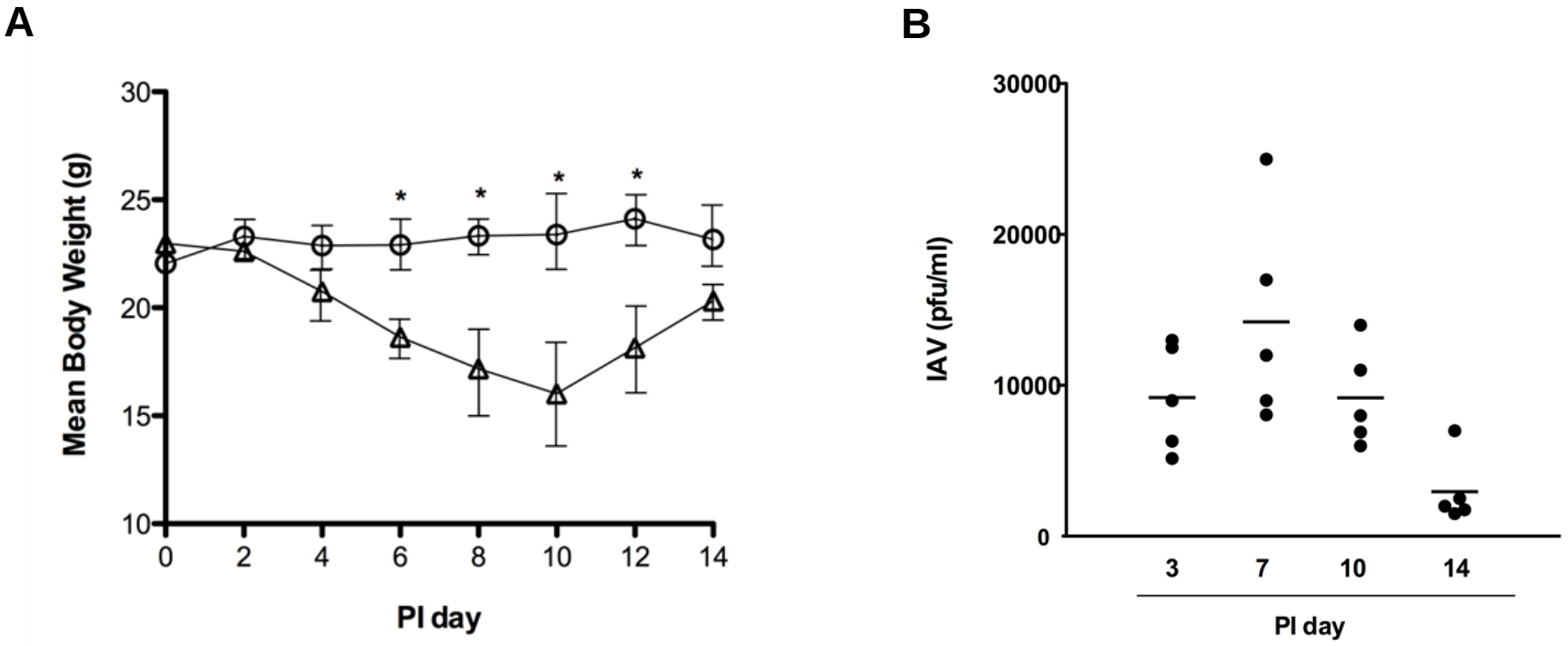

AJRCMB Articles in Press. Published on 09-March-2015 as 10.1165/rcmb.2014-0334OC

Figure 6

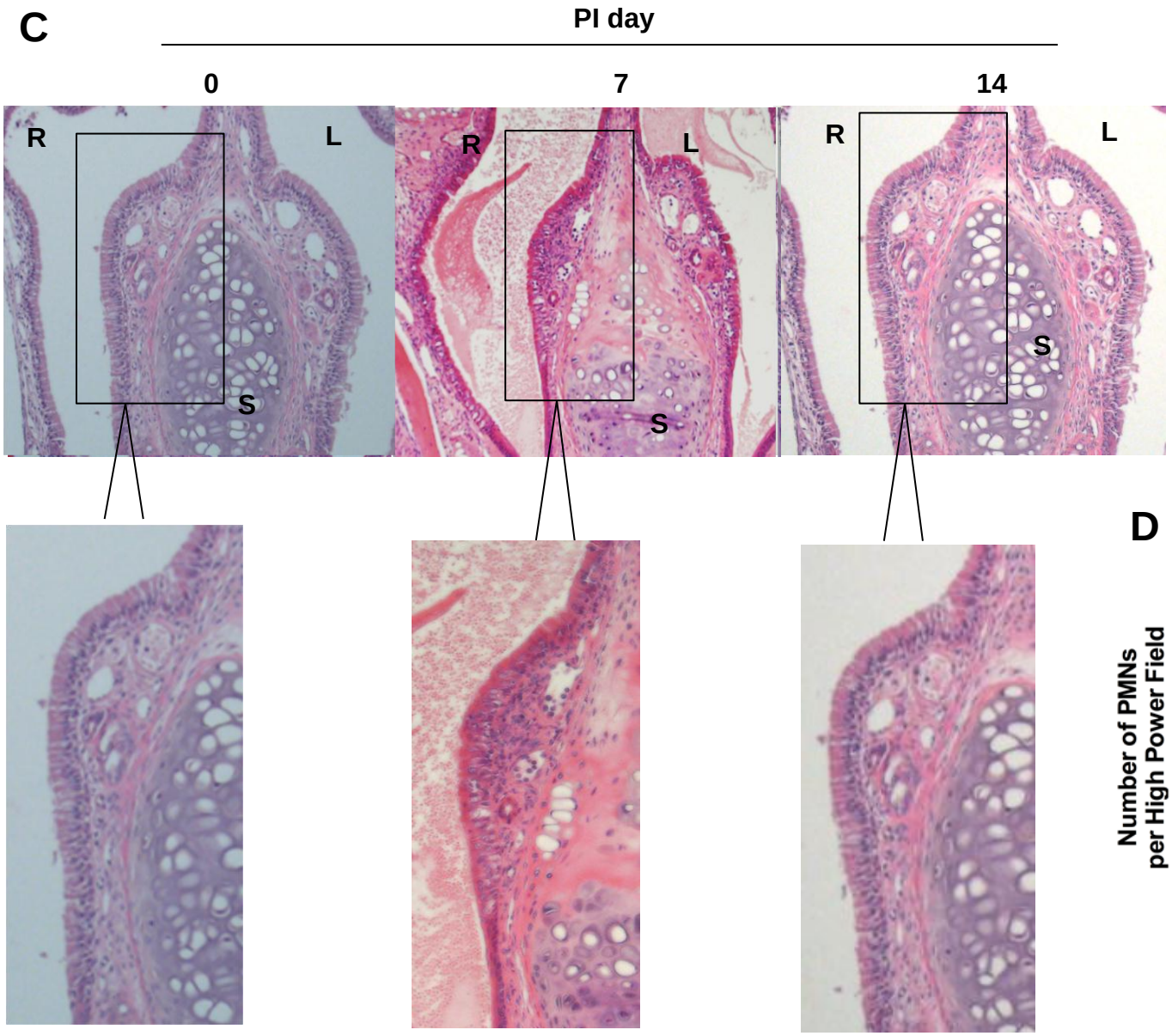

AJRCMB Articles in Press. Published on 09-March-2015 as 10.1165/rcmb.2014-0334OC

Figure 7

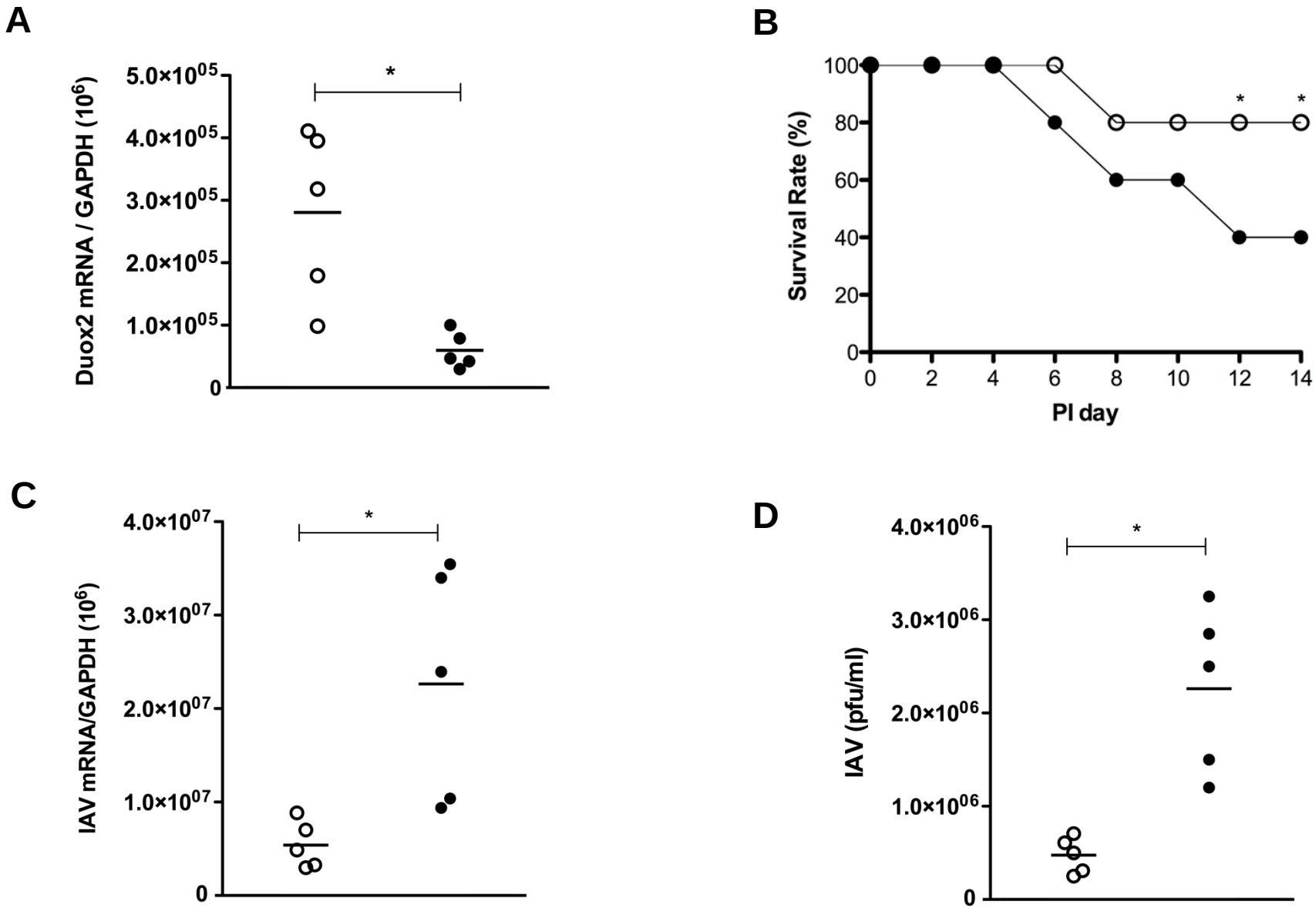

Figure 7

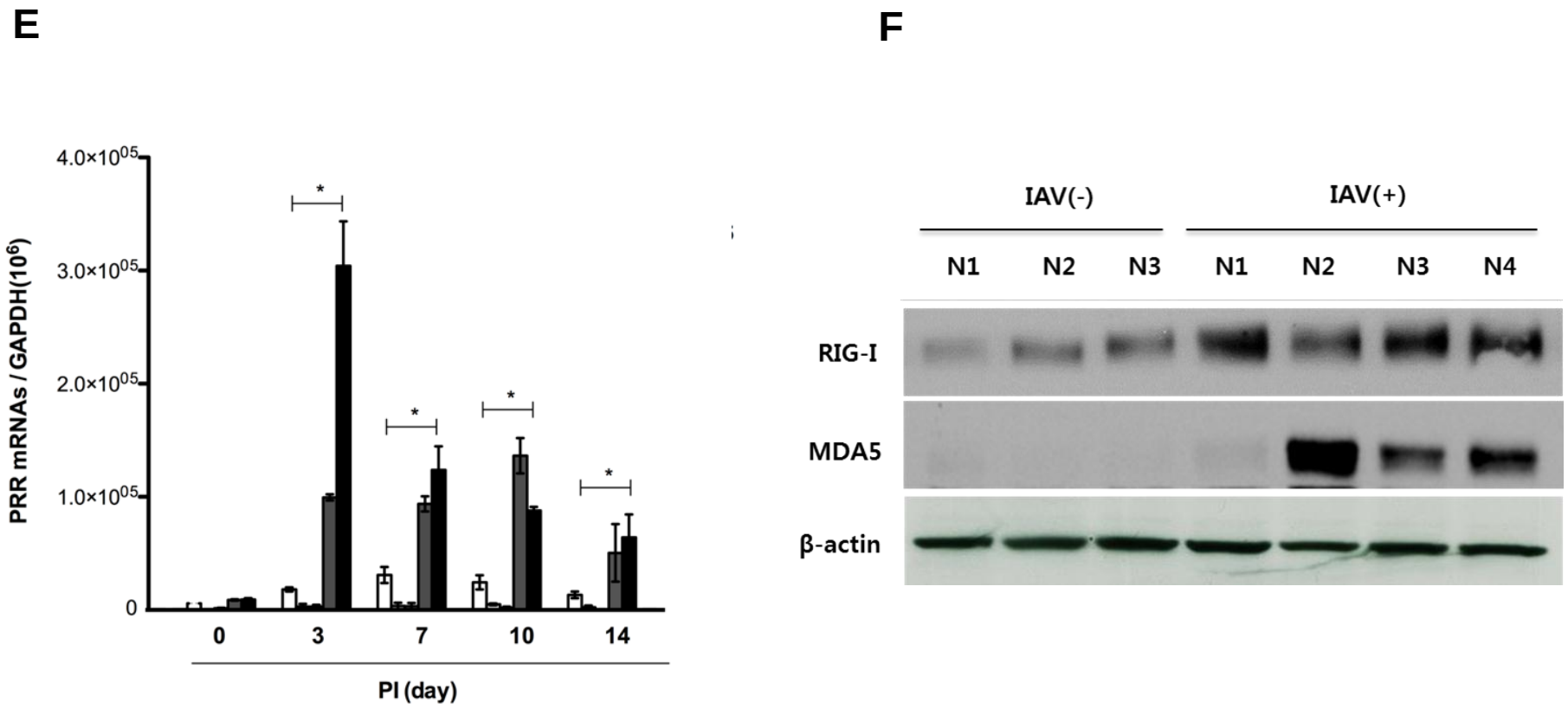

AJRCMB Articles in Press. Published on 09-March-2015 as 10.1165/rcmb.2014-0334OC

Figure 7

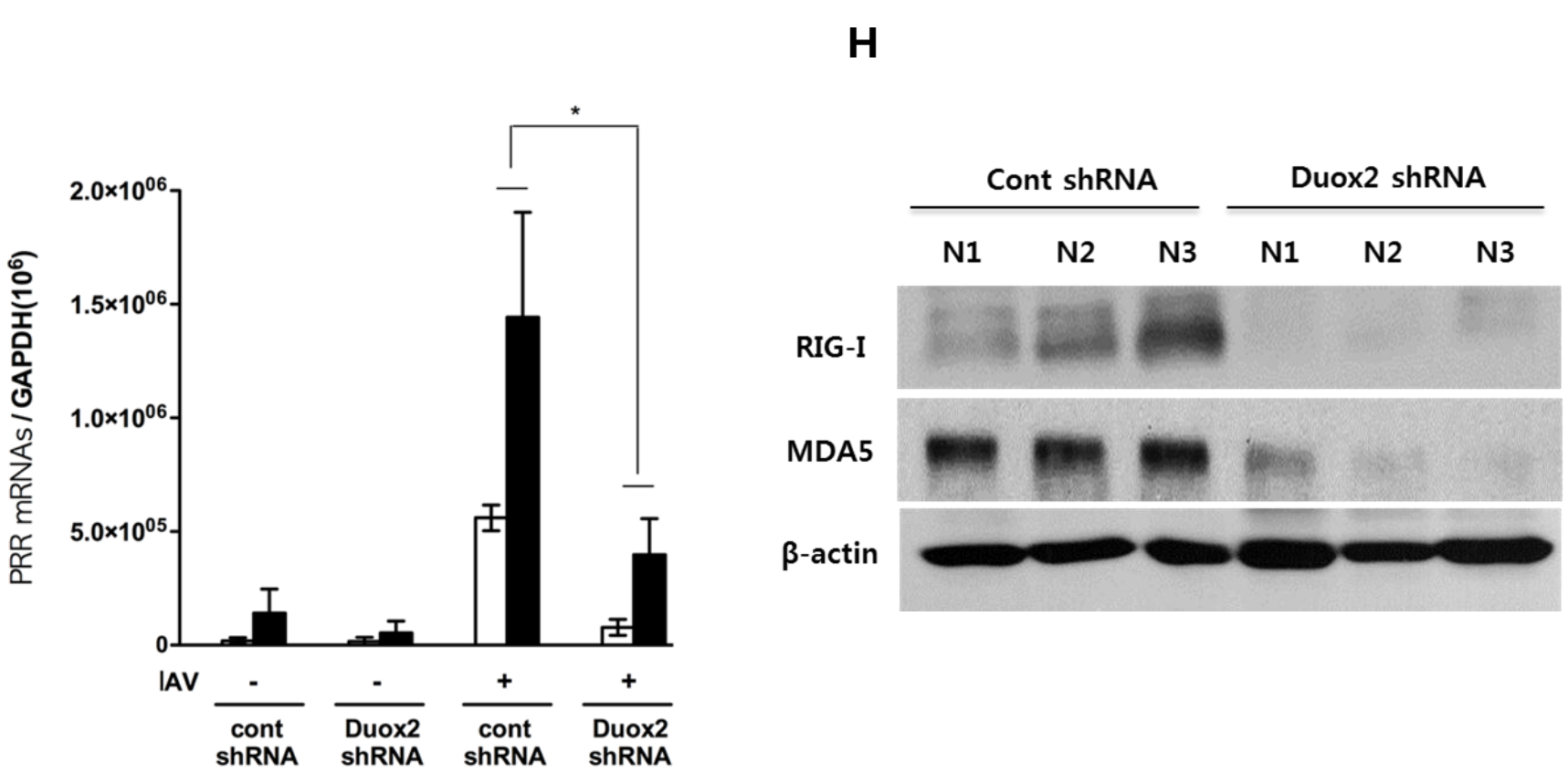

Figure 8

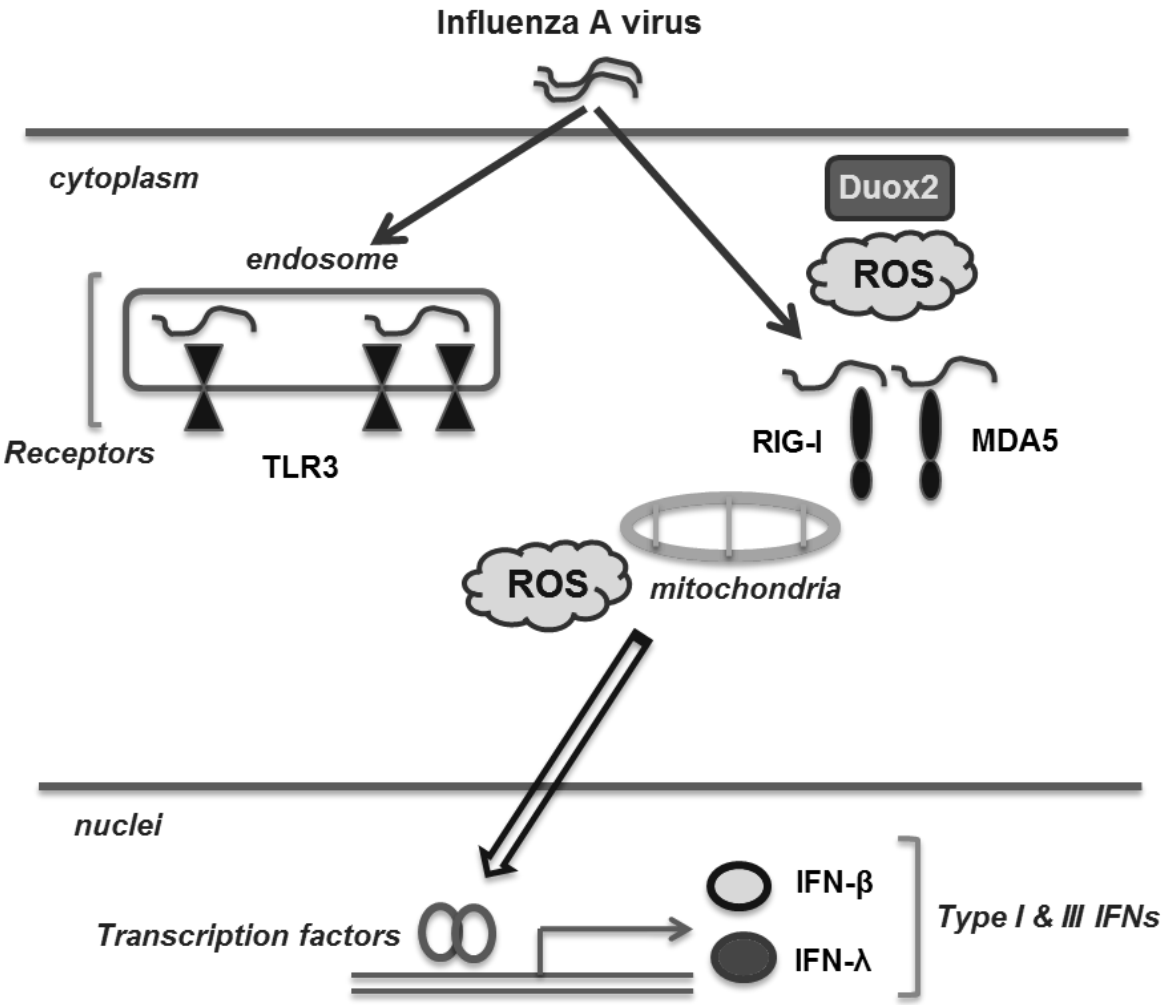

AJRCMB Articles in Press. Published on 09-March-2015 as 10.1165/rcmb.2014-0334OC

Online Supplement

Viruses and reagents

Influenza A/WS/33 virus (IAV WS/33: H1N1, ATCC, Manassas, VA, USA) was used to infect NHNE cells and mouse nasal mucosa. The virus was grown in Madin-Darby canine kidney (MDCK) cells with virus growth medium, according to the standard procedure (15). After 48-h incubation at 37°C, the supernatant was harvested and centrifuged at 5000 rpm for 30 min to remove cellular debris. Virus was titrated into MDCK cells using a tissue culture infectious dose assay, and virus stocks were stored at -80°C. Anti-β-actin antibody was purchased from Calbiochem (San Diego, CA, USA) and anti-IAV nucleoprotein antibody was purchased from Fitzgerald Industry International (North Acton, MA, USA). Short hairpin RNA (shRNA) containing lentiviral particles for Nox4, Duox1, and Duox2 were purchased from Santa Cruz Biotechnology (Santa Cruz, CA, USA). 2′,7′-Dichlorofluorescein diacetate (DCF-DA) was purchased from Life Technologies (Grand Islands, NY, USA), and anti-rabbit RIG-I and MDA5 antibodies were from Enzo Life Sciences, Inc (Farmingdale, NY, USA).

Cell culture

The Institutional Review Board of the Chung-Ang University College of Medicine approved this study (IRB number C20122095) and all adult subjects who participated in the study provided written informed consent. Specimens for the culture of NHNE cells were obtained from the middle nasal turbinate of five healthy volunteers. We cultured these specimens using a system designed for normal human nasal epithelial (NHNE) cells (14, 16). Briefly, passage-2 NHNE cells (1×10^5 cells/culture)

were seeded in 0.5 ml culture medium on Transwell-clear culture inserts (24.5 mm; 0.45-μm pore size; Costar Co., Cambridge, MA, USA). Cells were cultured in a 1:1 mixture of basal epithelial growth medium and Dulbecco's modified Eagle's medium containing previously described supplements. Cultures were grown submerged for the first nine days; the culture medium was changed on day one and every other day thereafter. An air-liquid interface (ALI) was created on day nine by removing the apical medium and feeding the cultures from the basal compartment only. The culture medium was changed daily after formation of the ALI. All the experiments described herein used NHNE cells at 14 days after ALI formation.

Mice

Male C57BL/6J (B6) mice (Orientalbio, Seoul, Korea) aged 7 weeks (19–23 g) were used as wild-type (WT), and All experiments were approved by the Institutional Review Board of the Yonsei University College of Medicine (IRB number 2014-0163).

Virus inoculation

Passage-2 fully differentiated NHNE cells were either mock-infected (PBS) or inoculated with IAV (WS/33, H1N1) to apical side of ALI at a multiplicity of infection (MOI) of 1. After a 2-h absorption period, the inoculum was aspirated, and cells were washed twice with culture medium. After washing, culture medium was replaced, and the cells were incubated at 37°C in 5% CO2. At the designated times post-inoculation, the culture supernatant was collected for virus titration using a TCID50 assay.

AJRCMB Articles in Press. Published on 09-March-2015 as 10.1165/rcmb.2014-0334OC

IAV (WS/33, H1N1; 213 pfu in 30 μl PBS) was inoculated into WT or Duox2 mutant mice by intranasal delivery. After euthanasia, nasal lavage (NAL) fluid was obtained from the mouse nasal cavity by lavaging with 1000 μl 0.5 mM ethylene diamine tetraacetic acid (EDTA) in phosphate-buffered saline (PBS) after cannulation of the choana (posterior end of nasal cavity). The collected NAL fluid was centrifuged at 1000 g for 10 min and the cell pellet was deposited onto glass slides using a Cytospin centrifuge (600 g for 5 min). The supernatant was stored at –80°C and the collected NAL fluid was used for the plaque assay. Mouse nasal mucosa which are attached to the nasal septum, were also harvested for real-time polymerase chain reaction (PCR), western blot analysis, and immunohistochemistry.

Western blot analysis

The NHNE cells and homogenized mouse nasal mucosa were lysed with 2× lysis buffer (250 mM Tris-Cl [pH 6.5], 2% sodium dodecyl sulfate [SDS], 4% β-mercaptoethanol, 0.02% bromophenol blue, and 10% glycerol). Lysates (30 μg protein) were electrophoresed in 10% SDS gels and transferred to polyvinylidene difluoride membranes in Tris-buffered saline (TBS; 50 mM Tris-Cl (pH 7.5), 150 mM NaCl) for 1 h at room temperature. The membrane was incubated overnight with primary antibody in Tween-Tris buffered saline (TTBS; 0.5% Tween-20 in TBS). After washing with TTBS, the blot was incubated for 1 h at room temperature with secondary anti-rabbit or anti-mouse antibody (Cell Signaling, Beverly, MA, USA) in TTBS and visualized using an enhanced chemiluminescence (ECL) system (Amersham, Little Chalfont, UK).

RT-PCR

Total RNA was isolated from NHNE cells infected IAV (WS/33, H1N1) with using TRIzol (Invitrogen). cDNA was synthesized with random hexamer primers (PerkinElmer Life Sciences, Waltham, MA and Roche Applied Science, Indiapolis, IN) using Molony murine leukemia virus-reverse transcriptase (PerkinElmer Life Sciences). Oligonucleotide PCR primers were designed based on the TLR3, TLR7, TLR9, RIG-I, MDA5, Duox2, and Duoxa2 Genbank TM sequences (Table E1). We used comparative kinetic analysis to compare the mRNA levels of each gene for each set of culture conditions as described previously (24). PCR products were resolved on 2% agarose gels (FMC, Rockland, ME) and visualized with ethidium bromide under a transilluminator. When reverse transcriptase was omitted, no PCR products were observed, confirming that the amplified products were from mRNA, not genomic DNA contamination. The specific amplification of target genes was confirmed by sequencing the PCR products (dsDNA Cycle Sequencing System; GibcoBRL, Rockville, MD).

Real-time PCR

Total RNA was isolated from NHNE cells and homogenized mouse nasal mucosa infected with WSN/33 (H1N1) at 10 and 30 min, 1, 2, and 8 h, 1, 2, 3, 7, 10, and 14 days using TRIzol (Invitrogen, Carlsbad, CA, USA). cDNA was synthesized from 3 μg of RNA with random hexamer primers using Moloney murine leukemia virus reverse transcriptase (PerkinElmer Life Sciences, Waltham, MA, USA and Roche Applied Science, Indianapolis, IN, USA). Commercial reagents (TaqMan Universal PCR Master Mix, PE Biosystems, Foster City, CA, USA) were selected and conditions were set according to the manufacturer's protocol. The total reaction volume of 12 μl contained 2 μl of cDNA (reverse transcription mixture),

AJRCMB Articles in Press. Published on 09-March-2015 as 10.1165/rcmb.2014-0334OC

oligonucleotide primers at a final concentration of 800 nM, and TaqMan hybridization probe at 200 nM. The real-time PCR probe was labeled at the 5' end with carboxyfluorescein (FAM) and at the 3' end with the quencher carboxytetramethylrhodamine (TAMRA).

Primers for human Nox4, Duox1, Duox2, TLR3, RIG-I (DDX58), and MDA5 (IFIH1) were purchased from Applied Biosystems (Foster City, CA, USA). Real-time PCR was performed using the PE Biosystems ABI PRISM® 7700 Sequence Detection System. The thermocycler parameters were 50°C for 2 min and 95°C for 10 min, followed by 40 cycles of 95°C for 15 s and 60°C for 1 min. Target mRNA levels were quantified using target-specific primer and probe sets for IAV WSN/33 (H1N1), Nox4, Duox1, Duox2, TLR3, RIG-I, and MDA5. All PCR assays were quantitative and utilized plasmids containing the target gene sequences as standards. All probes were designed to span an intron and did not react with genomic DNA. All reactions were performed in triplicate, and all real-time PCR data were normalized to the level of the housekeeping gene glyceraldehyde phosphate dehydrogenase (GAPDH, 1×10^6 copies) to correct for variations between samples.

The measurement of ROS

After stimulation with WS/33 (H1N1) for 10 and 30 min, 1, 2, and 8 h, and 1, 2, and 3 days, confluent cells were washed with RPMI (lacking phenol red). The cells were washed with 1 ml of Hanks' balanced salt solution at least five times to remove mucus secretion, and were then incubated with 5 μM of 2′,7′-DCF-DA for 10 min. Transwell-clear culture inserts were examined with a Zeiss Axiovert 135 inverted microscope equipped with a x20 Neofluor objective and a Zeiss LSM 410 confocal attachment (Minneapolis, MN, USA). The DCF fluorescence level was measured at

the excitation wavelength of 488 nm and the emission wavelength of 515–540 nm. Fluorescence intensities from seven randomly selected fields in each dish were measured with the Carl Zeiss vision system (KS400, version 3.0). The seven values were averaged to obtain the mean relative fluorescence intensity, and the means were compared for each well. All experiments were repeated at least three times (10).

Cell transfection with Nox4, Duox1, and Duox2 shRNAs

Expression of Nox4, Duox1, and Duox2 was suppressed using gene-specific shRNAs (lentiviral particles), and the transfection rates for shRNAs were determined to be greater than 70% in NHNE cells. The cells were transfected with each shRNA using the Oligofectamine^{TM} reagent following the manufacturer's instructions (Invitrogen, Carlsbad, CA, USA). The shRNA (10 μl, 1×10^4 infectious units of virus) and Oligofectamine^{TM} (1 μg) were mixed individually with the culture media. Transfection was then performed over a 48-h period in 12-well NHNE cell plates. This procedure did not affect cell viability, and after 48 h of transfection, cells were infected with IAV. This procedure was repeated with control shRNA, which was also purchased from Santa Cruz**.** The endogenous expression levels of the Nox4, Duox1, and Duox2 genes were partially suppressed using shRNA, which was confirmed by real-time PCR.

Duox2 overexpression using full length of cDNA clones

For Duox2 overexpression in NHNE cells, cells were transfected with the Duox2 (NM_177610) and Duoxa2 (NM_025777) mouse cDNA ORF Clones purchased from Origene (Beijing, China).

AJRCMB Articles in Press. Published on 09-March-2015 as 10.1165/rcmb.2014-0334OC

Histological analysis of mouse nasal mucosa

IAV-inoculated C57BL/6 mice were sacrificed after being anesthetized and were fixed using 10% formaldehyde. A coronal cut was made 1mm posterior to the eyes using a razor blade. In this manner, the dyes and maxilla including the sinonasal cavity were isolated for tissue processing. Specimens were then decalcified and embedded in paraffin. The paraffin-embedded nasal cavity was sectioned coronally by continuous microtoming at a thickness of 4 um. Histological changes of nasal mucosa after IAV infection were examined by means of hematoxylin and eosin staining for general morphology and inflammatory cell counting in subepithelial area including lamina propria. Histological analysis was performed by the examiner blinded to the experimental group and best five sections, as determined by the greatest septal mucosal area included in the section, were used for evaluation. PMNs were counted quantitatively and the results were expressed as the number of cells per high power field. Additionally, general morphology such as the degree of subepithelial consolidation, epithelial detachment and secretion of nasal cavity was also assessed by the examiner blinded to the experimental group and best five sections.

Plaque assay

Virus samples were serially diluted with PBS. Six-well plates of confluent monolayers of MDCK cells were washed twice with PBS then infected in duplicate with 250 µl each of different virus dilutions. The plates were incubated at 37°C for 45 min to facilitate virus adsorption. Following adsorption, the cells were overlayed with 1% agarose (Invitrogen) in complete MEM supplemented with TPCK trypsin (1 µg/ml)

and 1% fetal bovine serum. The plates were incubated at 37°C, and at two days post-incubation, plaques were fixed with 10% formalin.

Duox2 silencing using lentiviral shRNA in mouse nasal mucosa

For Duox2 silencing in mouse nasal mucosa using shRNA lentiviral particles (Thermo Fisher Scientific Inc, Waltham, MA, USA), mice were anesthetized with 50mg/kg Zoletil (Virbac Korea, Seoul, Korea) and 10mg/kg Rompun (Bayer AG, Leverkusen, Germany) and given either mouse Duox2 shRNA (clone ID V3LMM-425530) or scrambled shRNA lentiviral particle ($3x10^7$ TU/ml) twice for three days apart intranasally in a total volume of 30 ul. After 6 days, the mice were used for the experiments.

Statistical analyses

At least three independent experiments were performed with cultured cells from each donor, and the results are presented as the mean value ± standard deviation (SD) of triplicate cultures. Differences between treatment groups were evaluated by analysis of variance (ANOVA) with a *post hoc* test. Differences were considered significant at $p<0.05$.

AJRCMB Articles in Press. Published on 09-March-2015 as 10.1165/rcmb.2014-0334OC

Table E1. Polymerase chain reaction (PCR) experimental conditions and oligonucleotide sequences.

Product	Cycle	Annealing Temp (^{o}C)	Primer	Oligonucleotide Sequence
TLR3	33	55	Forward	CTC AGA AGA TTA CCA GCC GC
			Reverse	TTC TAG TTG TGG AAG CCA AGC
TLR7	33	60	Forward	ACG AAC ACC ACG AAC CTC AC
			Reverse	GGC ACA TGC TGA AGA GAG TTA C
TLR9	33	55	Forward	CAA CAA CCT CAC TGT GGT GC
			Reverse	GAG TGA GCG GAA GAA GAT GC
RIG-I	33	55	Forward	GCA TAT TGA CTG GAC GTG GCA
			Reverse	CAG TCA TGG CTG CAG TTC TGT C
MDA5	33	55	Forward	GTT GAA AAG GCT GGC TGA AAA C
			Reverse	TCG ATA ACT CCT GAA CCA CTG
Duox2	32	60	Forward	GGA CAG CAT GCT TCC AAC AAG T
			Reverse	GCC TGA TAA ACA CCG TCA GCA
Duoxa2	32	60	Forward	CGT TAA CAT TAC ACT CCG AGG AAC A
			Reverse	CAG AAT GCC ACC CAC AGT GT
*β2-M	23	55	Forward	CTCGCCCTACTCTCTCTTTCTGG
			Reverse	GCTTACATGTCTCGATCCCACTTAA

* β2-M: β2 microglobulin